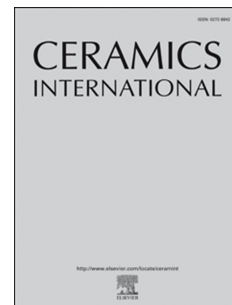


Journal Pre-proof

A comprehensive review of electric discharge machining of advanced ceramics

Wuyi Ming, Haojie Jia, Hongmei Zhang, Zhen Zhang, Kun Liu, Jinguang Du, Fan Shen, Guojun Zhang



PII: S0272-8842(20)31495-4

DOI: <https://doi.org/10.1016/j.ceramint.2020.05.207>

Reference: CERI 25308

To appear in: *Ceramics International*

Received Date: 9 March 2020

Revised Date: 1 May 2020

Accepted Date: 18 May 2020

Please cite this article as: W. Ming, H. Jia, H. Zhang, Z. Zhang, K. Liu, J. Du, F. Shen, G. Zhang, A comprehensive review of electric discharge machining of advanced ceramics, *Ceramics International* (2020), doi: <https://doi.org/10.1016/j.ceramint.2020.05.207>.

This is a PDF file of an article that has undergone enhancements after acceptance, such as the addition of a cover page and metadata, and formatting for readability, but it is not yet the definitive version of record. This version will undergo additional copyediting, typesetting and review before it is published in its final form, but we are providing this version to give early visibility of the article. Please note that, during the production process, errors may be discovered which could affect the content, and all legal disclaimers that apply to the journal pertain.

© 2020 Published by Elsevier Ltd.

A Comprehensive Review of Electric Discharge Machining of Advanced Ceramics

Wuyi Ming^a, Haojie Jia^{a,c}, Hongmei Zhang^c, Zhen Zhang^{b,*}, Kun Liu^a, Jinguang Du^a, Fan Shen^{a,c}, Guojun Zhang^c

^a*Henan Key Lab of Intelligent Manufacturing of Mechanical Equipment, Zhengzhou University of Light Industry, Zhengzhou, 450002, China*

^b*School of Aerospace Engineering, Huazhong University of Science and Technology, Wuhan, Hubei 430074, China*

^c*Guangdong HUST Industrial Technology Research Institute, Guangdong Provincial Key Laboratory of Digital Manufacturing Equipment, Dongguan, 523808, China*

Abstract

Advanced ceramics are widely used in high temperature and wear related situations due to their unique physical and chemical characteristics. With the increasing demand for ceramics, the machining techniques of ceramics become a hot and tough issue because ceramics are extremely fragile and difficult to process. Traditional mechanical machining techniques like milling, turning, and drilling are subjected to large cutting forces and heat leading to extensive tool wear and poor machining performance. **Electric discharge machining (EDM) has an outstanding ability of no-contact machining brittle and hardness materials with complex shapes via generating extreme high-temperature plasma channel to melt and vaporize materials.** Therefore, in this paper, the research trends of latest EDM technologies for advanced ceramic materials **were** comprehensively reviewed. Firstly, according to the electrical conductivity of advanced ceramics, different EDM processes **were** introduced in details. Secondly, the existing physical models and material removal mechanisms of EDM process of ceramics **were** compared and analyzed. Then the machining performance indicators, such as MRR, Ra, TWR, surface topography, and micro-structures, **were** respectively investigated. Additionally, the new hybrid machining techniques of EDM **were** presented to provide some potential for efficiently machining advanced ceramics. Eventually, this paper also **discussed** the challenges associated with electrical discharge machining of advanced ceramic materials, and **suggested** some related research areas which possibly attract significant research attentions in the future.

Keywords: Electric discharge machining, ceramic materials, physical models, material removal mechanism, machining performance indicators, hybrid machining

1. Introduction

Compared with metal and polymer materials, advanced ceramic materials are more suitable for wear and high temperature applications because of their physical and chemical properties, with which chemical reactions are not easy to perform. In addition, due to its high hardness, high strength, low thermal conductivity and biocompatibility, excellent chemical stability and wear resistance, ceramic materials **were** more and more popular, not only in the tool industry, but also in aerospace and biomedicine [1, 2, 3, 4, 5]. Figures 1a~ i depict the application of advanced ceramic materials in engineering field. For example, the high-speed cutting tools made of silicon nitride ceramics **accounted** for 1/3 of the total number of ceramic cutting tools [6, 7, 8]. Their cutting ability and wear resistance exceeded the best cemented carbide tools, and their cutting speed **was** 3-10 times higher than that of cemented carbide. In the field of aerospace, silicon nitride ceramic bearings **had** excellent high-speed performance. When they **were** used in precision ceramic bearings, their manufacturing accuracy can reach up to P4 level. A bearing made of silicon nitride ceramics is shown in Fig.1f [9]. The requirements of manufacturing high-quality micro-systems can be answered by

*Corresponding author.
E-mail address:jameszhang198808@gmail.com

properties of advanced ceramics, because mechanical components of these micro-systems are often exposed to high temperature and mechanical loads. In the biomedical field, because the materials prepared by ZrO_2 or Al_2O_3 had strong and stable biological inertia, this kind of ceramics can be used make dental implants and prostheses, bone clips and scaffolds for tissue engineering [4, 10, 11, 12, 13], as shown in Fig.1h. Moreover, the Si_3N_4 -TiN gas turbine impeller (in Fig.1a), Si_3N_4 /multi-walled carbon nanotubes(MWCNTs) micro gear (in Fig.1e), example of Si_3N_4 arbitrary shape part (in Fig.1i) could be made by micro-electrical discharge machine (micro-EDM), EDM, and wire-EDM (WEDM),respectively. As depicted in Fig.1b, the workpiece ($SiSiC$) with complex features could be also fabricated by the EDM process.

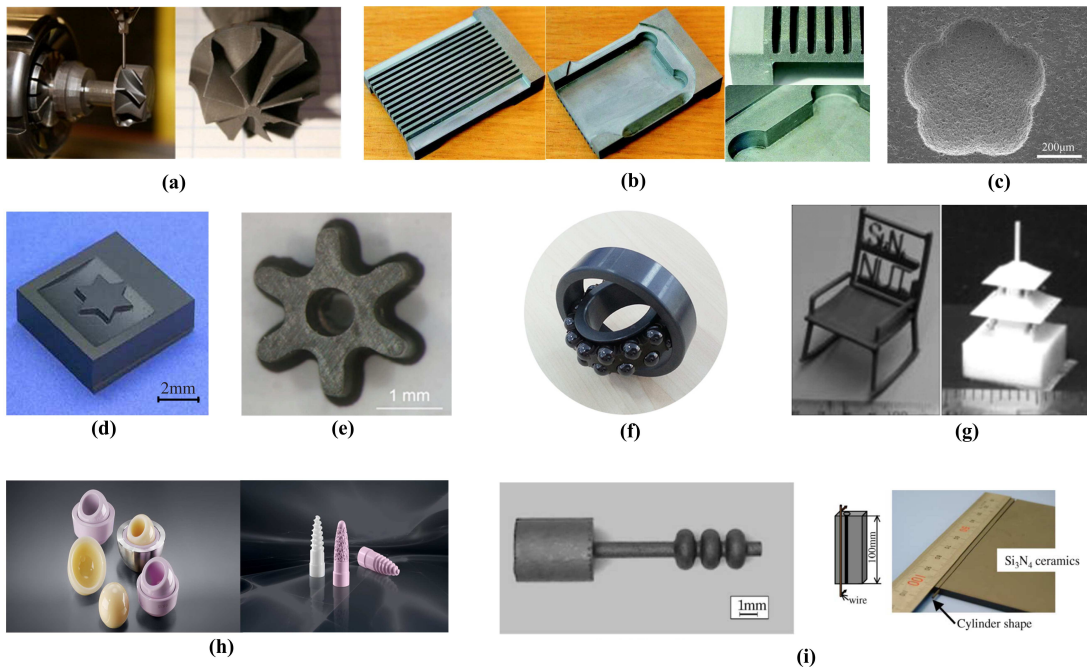


Figure 1: Application of advanced ceramic materials; (a) Si_3N_4 -TiN gas turbine impeller milled by micro-EDM [14]; (b) A workpiece ($SiSiC$) with complex features by EDM [15]; (c) SEM images of micro-cavies fabricated by micro-EDM [16]; (d) A sample of insulating Si_3N_4 advanced ceramics by EDM [17]; (e) Optical image of Si_3N_4 / MWCNTs micro gear by EDM [18]; (f) Silicon nitride ceramic bearing (ferrule and rolling elements) in aerospace [9]; (g) Examples of chair shape (Si_3N_4) and temple (ZrO_2) products by WEDM [19]; (h) dental ceramics and joint replacement (Al-based) in biomedicine [20]; (i) Examples (Si_3N_4) of cylinder shape and arbitrary shape by WEDM [21].

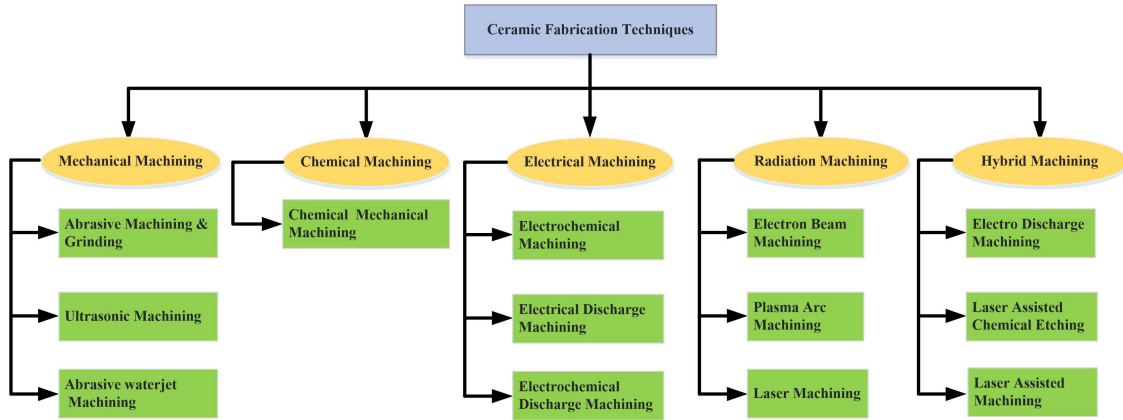
Advanced ceramic materials are mainly divided into conductive and non-conductive according to the conductive situation. Commonly used silicon carbide (SiC), alumina (Al_2O_3), silicon nitride (Si_3N_4), and zirconia (ZrO_2) advanced ceramics are non-conductive materials. Titanium diboride (TiB_2), zirconium diboride (ZrB_2), boron carbide (B_4C), metal nitrides (TiN and ZrN) and other similar ceramic materials are natural conductors. By adding conductive particles such as TiC , TiN , CaO , Si , TiB_2 or B_4C , Si_3N_4+TiN , Si_3N_4+TiC , Al_2O_3+TiC , Al_2O_3+TiN , and ZrO_2+CaO , $ZrO_2+Y_2O_3+TiN$ and other similar advanced ceramic materials could also become conductive materials [22, 23]. Table 1 shows the properties and application of different advanced ceramic materials.

However, the traditional machining method was also hindered because of the high hardness and brittleness of advanced ceramics. Considering the main shortcomings of its processing performance, the expense of polishing stage dominated the majority of the whole manufacturing costs. In addition, the traditional machining methods would damage the surface of advanced ceramic materials, resulting in cracks and stress concentration, which would affect mechanical strength of components. Therefore, the key step of advanced ceramic parts manufacturing was how to obtain low-cost effective processing techniques. Figure 2 summarizes the different machining techniques of advanced ceramic materials [33].

Table 1: Properties and applications of different advanced ceramic materials

Advanced ceramics	Performance properties	Class	Applications
SiC	High thermal conductivity, high temperature resistance, good wear resistance and chemical stability.	Non-Conductive	Bulletproof armor, missile tail nozzle, gas turbine blades, seals, bearings, shaft sleeves and other parts [24, 25, 26].
Al ₂ O ₃	Thermal stability, chemical stability, piezoelectricity, corrosion resistance, light transmittance, etc.	Non-conductive	Integrated circuit chip, spark plug, laser material, artificial bone, bearing, and mechanical precision parts [27].
Si ₃ N ₄	Good high temperature resistance, thermal shock resistance, wear resistance, and corrosion resistance.	Non-conductive	Widely used in the field of aeronautics and astronautics, such as new type of transparent materials [28].
ZrO ₂	Excellent electrical conductivity, wear resistance, high temperature resistance, corrosion resistance and biocompatibility.	Non-conductive	Thermal barrier coating, catalyst carrier, medical treatment, refractory, textile and other fields [29, 30].
ZrB ₂ , TiB ₂	High melting point, hardness, oxidation resistance and wear resistance.	Conductive	Wear-resistant, corrosion-resistant coating, evaporation boat or container, film capacitor, optical device film and high-temperature engine [31].
TiN, ZrN	Good mechanical, chemical, electrical, and thermal properties.	Conductive	Cutting tools, high temperature molds and abrasives, electronic substrate materials [24].
Al ₂ O ₃ + TiC, Al ₂ O ₃ + TiN	Good thermal shock resistance and toughness.	Conductive	Cutting tools [24, 32].

Most traditional machining techniques made ceramics machining impossible or challenging [34], and also beared severe tool wear related to high cutting force, as well as longer cutting time and higher machining cost. Therefore, the traditional machining process did not seem to be suitable for ceramic manufacturing [35]. After the advanced ceramic materials were processed by abrasive machining & grinding, the products of these materials are easy to produce surface cracks, crushed layers, plastic deformation and significant residual stress [36, 37]. As the removal mechanism of ultrasonic machining advanced ceramic materials has not been fully studied, it was very difficult to optimize the process to obtain high-quality machining surface [38]. In abrasive water-jet machining, the surface fracture of advanced ceramic materials led to the formation of the slit because of the hydrodynamic effect. Since there was a certain fluctuation in the kerf width in the abrasive water-jet machining, however, the machining accuracy needs to be further enhancing [39]. Because of its impact on the environment, chemical machining [40, 41] was considered to be an unfriendly environmental process. Other non-contact processes such as laser machining [42, 43, 33], plasma machining [44, 45], electron beam machining [46, 47], and hybrid machining [48, 49, 50] also had their advantages and disadvantages as reported by different researchers. Therefore, for the processing of advanced ceramic materials, non-contact method has attracted more and more attentions. Electric discharge machining (EDM) has an outstanding ability of no-contact machining of difficult to process materials with complex shapes via generating pulse discharge channel of more than 10k degree to melt and vaporize materials. Table 2 shows the performance and relative comparisons of different machining processes.

**Figure 2:** Ceramic fabrication techniques for advanced ceramics [33].**Table 2:** Relative comparisons of different machining processes [33, 51]

Machining process	Economy and performances						
	Capital investment	Toolings \ fixtures	Power requirements	Tool wear	Removal efficiency	Structure dimensions	Surface quality
Traditional machining	Low	Low	Low	Low	Very Low	Middle	Low
Ultrasonic machining	Low	Low	Low	Medium	High	Small	Low
Electro chemical machining	Very high	Medium	Medium	Very Low	Low	Large	Medium
Chemical machining	Medium	Low	High	Very Low	Medium	Large	Medium
Electrical-discharge machining	Medium	High	Low	High	High	Middle	Medium
Plasma arc machining	Very low	Low	Low	Very low	Low	Small	High
Laser machining	Medium	Low	Low	Very low	High	Middle	Low

At present, the demand for sustainable manufacturing through environmentally-friendly is growing. Laws and regulations of various countries also put forward new requirements for green manufacturing. For example, the environmental management system (ISO 14000 standard) has been constantly implemented in Chinese enterprises, and many related manufacturing enterprises have begun to focus on the application of environmentally friendly processing techniques. In the process of EDM, deionized water and **kerosene** play the role of insulation and cooling consume less. In addition, by adopting the dry EDM method, the technique **could** be enhanced to a completely environmental-friendly manufacturing process [52, 53, 54]. Therefore, the EDM process of advanced ceramics is an important and

popular processing technique.

Considering the importance of the machining of advanced ceramic materials, this paper systematically summarizes the EDM techniques for advanced ceramics, the theoretical models and removal mechanism of EDM, the machining performance indicators of EDM, and the new hybrid machining techniques of EDM. In Section 2, a review over existing EDM techniques and applications is proposed in detail. Various machining techniques, such as traditional EDM, EDM with assisted electrode (prefabricated electrode technique and magnetic powder technique), and ECDM composite technique, for different conductive and non-conductive ceramics are introduced. In addition, the comparative analysis of these different methods is reviewed. Moreover, the theoretical models and removal mechanism of electrical discharge machining advanced ceramics are reviewed in Section 3. Furthermore, the machining performance indicators, such as material removal rate (MRR), surface roughness, tool wear ratio (TWR), surface topography, and micro-structures, are discussed in Section 4. Then, the specific discharge energy (SDE) is implemented to evaluate the performance of machining efficiency and difficulty level, which is most important to process advanced ceramics in the EDM. Lastly, new hybrid machining techniques and methods for advanced ceramics are analyzed and the application prospects are also presented in Section 5. Finally, some problems that should be further focused on are proposed, and the possible development trends of EDM process of advanced ceramics are forecasted in the future. The overall detailed outline of this review on EDM process of advanced ceramics is illustrated in Figure 3.

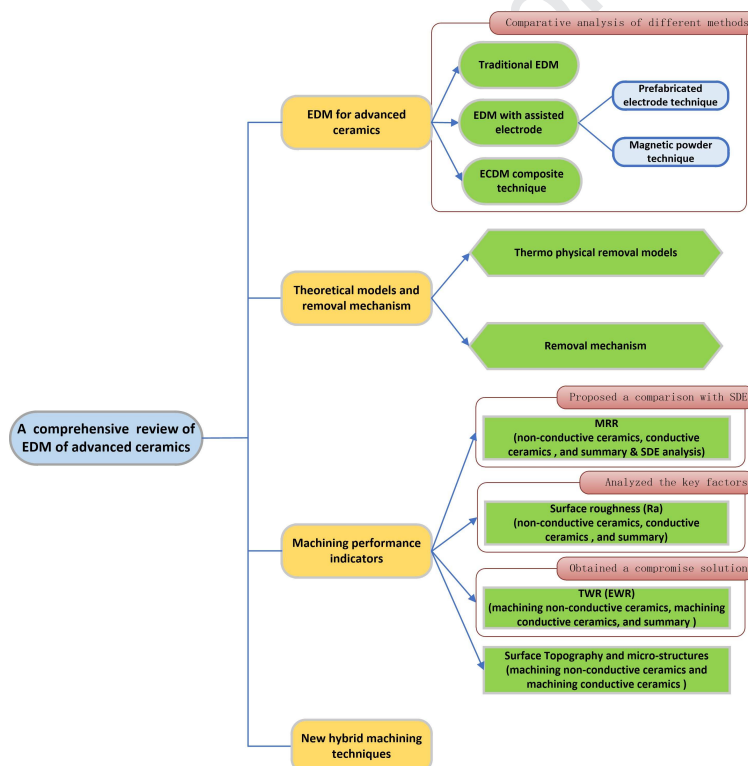


Figure 3: Overall diagram of the comprehensive review on EM machining of advanced ceramics.

2. EDM for advanced ceramics

EDM requires that machined materials have certain conductivity. Conductive advanced ceramics can be processed by the process by traditional EDM, but semiconductor and non-conductive advanced ceramics pose a considerable challenge to the process. Therefore, EDM with assisted electrode technique (EDM-AE) and EDM with other machining techniques make it possible to cutting these advanced ceramics.

2.1. Traditional EDM

Figure 4 shows the diagram of machining conductive advanced ceramics by traditional EDM. In the EDM process, the conductive tool electrode with the required geometry is close to the workpiece, but there is a certain gap between the workpiece and the electrode. Both the workpiece and the electrode, especially the gap between them, are submerged in working fluid (kerosene). The discharge voltage is employed between the electrode and the workpiece, which results in dielectric breakdown and a series of sparks. Then, a large amount of heat is generated, and the material on the workpiece and the electrode is melted and evaporated. Furthermore, the working fluid (kerosene) not only cools the electrode and the workpiece, but also brings out the debris between the discharges gaps to avoid short circuit during the discharge process.

It can be drawn from Table 1 that conductive ceramics such as zirconium diboride (ZrB_2), titanium diboride (TiB_2), zirconium nitride (ZrN) and titanium nitride (TiN) could be easily cut by traditional EDM, which was similar to other metal materials [55, 56]. However, the higher value of electrical conductivity ($> 10^{-2}/\Omega \cdot cm$) of advanced ceramics causes that the traditional EDM cannot perform in this situation. For example, non-conductive ceramics in Table 1, such as aluminum oxide (Al_2O_3), silicon carbon (SiC) or silicon nitride (Si_3N_4), do not meet the requirement. To solve this problem, a second conductive phase material was introduced to ceramics, which makes EDM process of insulating ceramics possible. A successful approach was implemented for traditional EDM to process silicon nitride (Si_3N_4), since the second conductive phase material (TiN) was incorporated into the advanced ceramics [57]. However, there was a disadvantage of this method, that is, the reinforcement material will affect the mechanical properties of the original ceramics. For example, there was a negative impact on the hardness, fracture toughness and bending strength of ZrO_2 when increasing the content of TiN added into ZrO_2 as second conductive phase[57].

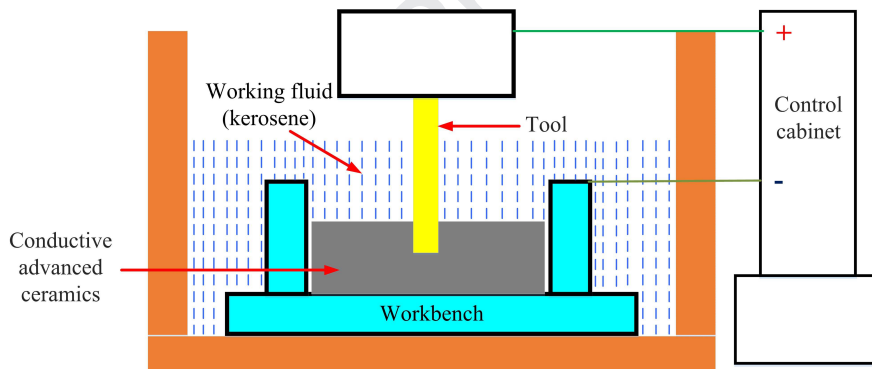


Figure 4: Diagram of machining conductive advanced ceramics by traditional EDM.

2.2. EDM with assisted electrode

EDM must produce spark discharge between the tool electrode and workpiece electrode, and machining of non-conductive advanced ceramic materials should also follow this principle. Therefore, it is necessary to make an auxiliary conductive electrode on the surface of the non-conductive material as the workpiece, so that it can generate spark discharge. The auxiliary electrode can be a metal, carbon and other conductive films which can be formed on the surface of the processed material (non-conductive advanced ceramics) through evaporation, coating and other methods, or can be magnetic powders, a metal plate and other conductive materials pressed on the surface of the processed material (non-conductive advanced ceramics).

2.2.1. Prefabricated electrode technique

When machining the interface of metal and non-conductive advanced ceramics with EDM, Mohri found that one side of metal was machined and eroded, and the other side of insulating ceramics was also machined and eroded[58]. Therefore, the non-conductive advanced ceramics could be cut by EDM with auxiliary electrode, and the principle is shown in Fig.5. Kerosene was used as working fluid, and the instantaneous high temperature produced by spark

discharge made kerosene dissociated carbon deposit on the surface of non-conductive advanced ceramics, and continuously produces conductive film so as to electric spark process of the ceramics. Using the auxiliary electrode technique, Tani and Mohri carried out wire-EDM (WEDM) of silicon nitride ceramics[59]. They studied the influence of different wire electrode materials (galvanized brass and molybdenum) on the MRR and surface roughness. They found that when the peak current was small, the MRR and surface roughness of galvanized brass wire were smaller than that of molybdenum wire. When the peak current was high, the removal rate of molybdenum wire was high but the surface roughness was also high. Fukuzawa studied the effect of open circuit voltage on the WEDM of zirconia ceramics[60]. And the results showed that the thickness of the conductive film increased with the increase of the open circuit status.

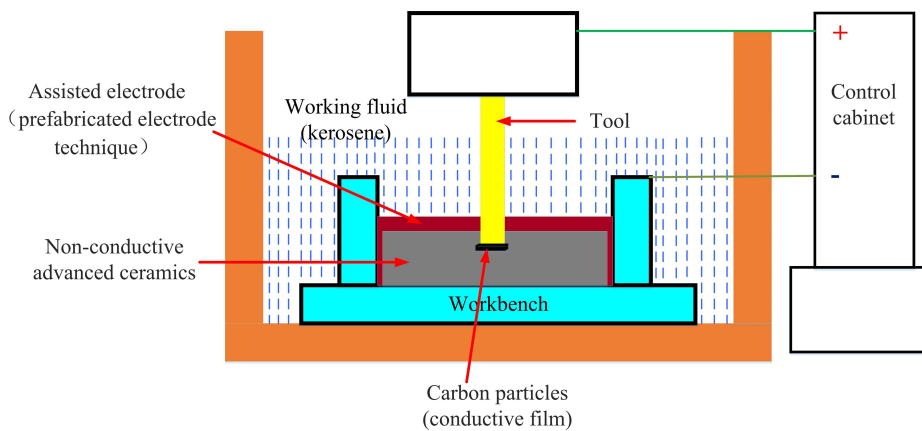


Figure 5: Diagram of machining non-conductive advanced ceramics by EDM with prefabricated electrode technique (EDM-PE).

Muttamara et al. studied the effect of different electrode materials on the EDM of Al-based ceramics[61]. Compared with copper and graphite electrode, the copper-infiltrated-graphite (EDM-C3) electrode had higher MRR ($0.11\text{mm}^3 / \text{min}$) and lower surface roughness ($\text{Ra} = 25\mu\text{m}$). When the positive electrode was used, the MRR of EDM-C3 electrode was 60% higher than that of the negative electrode, and the surface roughness (Ra) was decreased by 12% in this cutting settings. Praneetpongprung et al. studied the effect of an ultrasonic vibration combined with ED machining (USEDMD) Si_3N_4 ceramics[62]. The results showed that the amplitude of ultrasonic wave affected the formation of conductive film. Compared with non-ultrasonic vibration assist, the MRR of USEDMD composite machining was increased about 2 times, and the surface roughness increased with the increase of ultrasonic vibration. Kucukturk et al. carried out EDM research on Al_2O_3 , ZrO_2 , SiC , B_4C and other advanced ceramics, respectively[63]. The results showed that the processing time of Al_2O_3 ceramics was the longest, and the machining status was unstable; the processing time of ZrO_2 ceramics was the shortest, and the machining status was the most stable. In addition, it was also found that the use of internal flushing fluid can make it easier to cut these non-conductive advanced ceramics and improve the machining status. However, it also caused machining debris accumulated on the inlet hole easily leads to second discharges close to inlet hole, which perhaps enlarge the hole's diameter.

2.2.2. Magnetic powder technique

Figure 6 draws the diagram of machining non-conductive advanced ceramics by EDM with magnetic powder technique. The magnetic field generated by the magnet device went through the advanced non-conductive ceramics, which made the conductive magnetic particle attach to the surface of the ceramics, and formed the electrode pair with the tool electrode, resulting in the initial discharge condition [64]. When a pulse voltage is applied at both ends of the electrode and the conductive magnetic powder, a pulse discharge is generated at the place of the point of most easily breakdown between the two electrodes. Due to the effect of penetration and transmission, the discharge heat energy through the conductive magnetic powder will melt and vaporize the ceramics surface to form a discharge corrosion pit, so that the part of the workpiece material is processed. With the progress of the discharge, the conductive magnetic

powder is always adsorbed on the discharge surface of the ceramics by the magnetic force, and the carbon evolution is attached on the surface of the ceramics, forming a mixed conductive layer mainly composed of the conductive magnetic powder, the carbon evolution and the electrode material.

Xu used auxiliary electrode method (with magnetic powder technique) to process non-conductive SiO_2 ceramics in EDM [65]. It was found that low voltage and low current should be used as much as possible in the initial processing stage. In this way, a stable carbon conductive film could be formed on the processing surface before the auxiliary electrode penetrates, so as to ensure the continuous and stable machining in the EDM process. In addition, graphite electrode **could** enhance the conductivity of the conductive film and improve the processing stability [65].

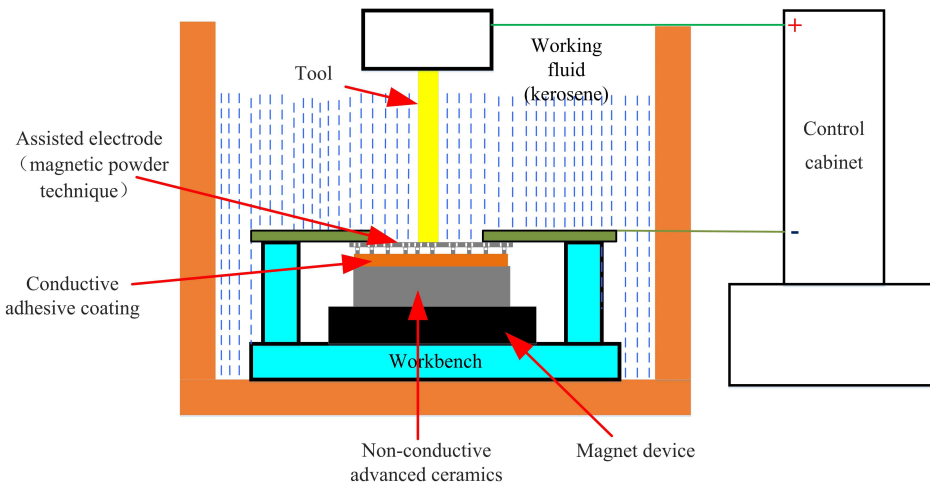


Figure 6: Diagram of machining non-conductive advanced ceramics by EDM with magnetic powder technique (EDM-MP).

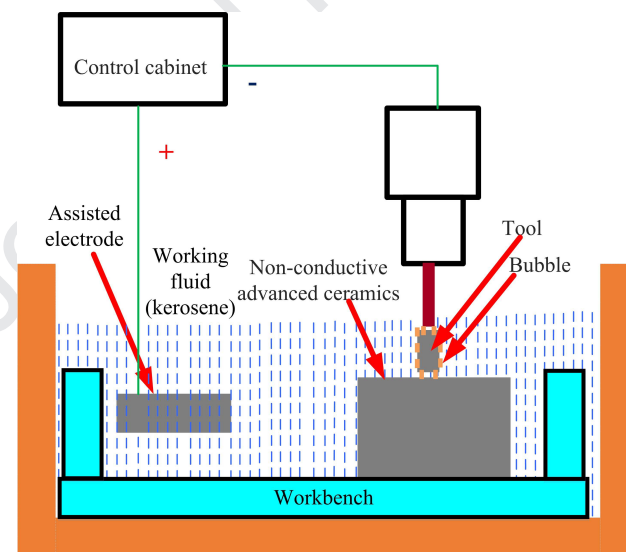
2.3. ECDM technique

The electrochemical discharge machining (ECDM), a hybrid machining technique, is applied for insulating materials. Its processing principle is shown in Fig.7. This method uses electrochemical reaction to form a gas non-conductive phase on the surface of tool electrode, resulting in a high potential difference between tool electrode and working fluid. When the potential difference is high enough to break down the gas (non-conductive phase), an electric spark is generated to remove the workpiece material. Tsutsumi et al. used pulse power supply and steel electrode with diameter of 0.5mm, in NaOH , NaNO_3 and NaCl electrolytes, to carry out the experimental research on the drilling of holes for insulating alumina ceramics, and found that the processing efficiency was the highest in NaOH electrolytes [66].

In the process of ECDM, the actual removal of non-conductive advanced ceramics is spark discharge, while the electrolysis is used to produce gas (non-conductive phase) and high potential difference. However, the electrolysis consumes a large amount of energy to form gas (non-conductive phase) by electrochemical effect, resulting in lower machining efficiency. Thereafter, Liu et al. studied the mechanism of ECDM by gas-filled electro-discharge technique, replacing the electrochemical film with physical gas. This new process **could** shorten the preparation time of discharge and improve the machining efficiency [67]. In addition, it was also found that NaOH was the most suitable electrolyte for Al_2O_3 and ZrO_2 , while NaNO_3 **was** the most suitable electrolyte for Si_3N_4 .

Table 3: Comparisons of different techniques assisted EDM for cutting advanced ceramics

Methods	Economy and performances				
	Cutting materials	Expense	Processing stability	Removal efficiency	Environmental impact
Traditional EDM	Conductive advanced ceramics	Low	High	High	Low
EDM-AE technique	\	\	\	\	\
EDM-PE	Non-conductive advanced ceramics	Low	Low	Low	Low
EDM-MP	Non-conductive advanced ceramics	Medium	Medium	Low	Low
ECDM technique	Non-conductive advanced ceramics	High	Medium	Medium	High

**Figure 7:** Diagram of machining non-conductive advanced ceramics by ECDM with magnetic powder technique.

2.4. Comparative analysis of different methods

In this subsection, different techniques assisted EDM for cutting advanced ceramics are compared, which are listed in Table 3. It is well known that the traditional EDM can only cut the conductive advanced ceramics, which is described in subsection 2.1. The key to cut non-conductive advanced ceramics is the preparation of auxiliary electrode in EDM. The effect of using gold coating as auxiliary electrode is better than using metal mesh or plate. New conductive films are formed on the machined surface of non-conductive advanced ceramics by EDM with auxiliary electrode

technique. In the actual processing, however, the natural generation of conductive film and the ceramic surface depositions is not uniform, since the main components of the conductive film are carbon and its carbonic compounds. The thickness of film is not uniform, and its bonding performance is poor. Hence, it is easy to peel off during machining, which often leads to unstable discharge. Although the removal efficiency of ECDM technique is much better than that of EDM with assisted electrode, the environmental impact of former is more serious than that of latter because of the treatment of electrochemical waste. Moreover, the expense of ECDM technique is the most considerable in these four techniques.

3. Theoretical models and removal mechanism

3.1. Thermo physical removal models

It is one of the hotspots of EDM to study the simulation by thermal physical removal models. The influence of temperature distribution and electrical parameters on machining performance is the main purpose of finite element study, and many researchers have made contributions to it. In the EDM process, the mainstream thermo physical removal models are shown in Fig.8.

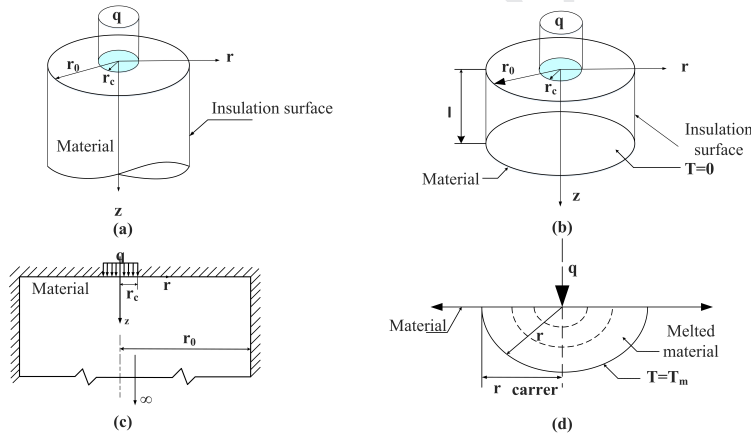


Figure 8: Thermo physical removal models for the process of EDM; a) Snoey's heat source model [68]; b) Dijck's heat source model [69]; c) Beck's heat source model [70, 71]; d) Dibitonto's heat source model [72].

Snoeys proposed a disk heat source model (in Fig.8a), which was used to simulate the heat source input to the cathode surface [68]. The outer area of the cathode was assumed to be insulated, and the heat source was assumed to active all the time during the conduction of the pulse-on. Considering the actual processing situation, Dijck [69] modified the disk heat source model proposed by Snoeys [68], and assumed that the electrode length in z-axis direction of heat source input should be infinite (finite length in Snoeys model), as shown in Fig.8b. Moreover, the model proposed by Beck [70, 71] is shown in Fig.8c. The proposed model considered that the electrode material surface was heated by the heat source centering on the disk-shaped area. Except for the area of energy input, all other parts of the material surface were thermally insulated. Because the model was not specially established for EDM process, however, a small part of the heat source was not transferred to the cathode. Therefore, Jilani [73, 74] had improved the simulation accuracy based on the theoretical model, which was proposed by Beck [70, 18]. Considering that the radius of plasma channel at the cathode was assumed to be much smaller than that at the anode, the model proposed by Dibitonto [72] considered that it was more reasonable for the heat flux to follow the Gaussian distribution. In addition, the energy distribution to the cathode was 18% of the total energy in this model, rather than 50% of the disk heat source model, as shown in Fig.8d

3.1.1. Non-conductive ceramics

Based on the heat conduction theory, Yu established a finite element model (with Gaussian distribution of heat flux [72]) of single pulse discharge for EDM with assisted electrode of non-conductive advanced ceramics, and calculated the three-dimensional temperature field of tool electrode, auxiliary electrode and **non-conductive advanced ceramics** [75]. The simulation results are shown in Fig.9. As the heat on the electrode and ceramic workpiece was too late to conduct the inside of them, the highest temperature appearing on the auxiliary electrode (copper strip) was 10405°C. Moreover, the highest temperature on the ceramic surface reached 9688°C, and the highest temperature of the electrode was 10332°C. The simulation results showed that the temperature on the advanced ceramics also increased with the increase of pulse-on time, which leaded to the increase of the melting area and vaporization area [75].

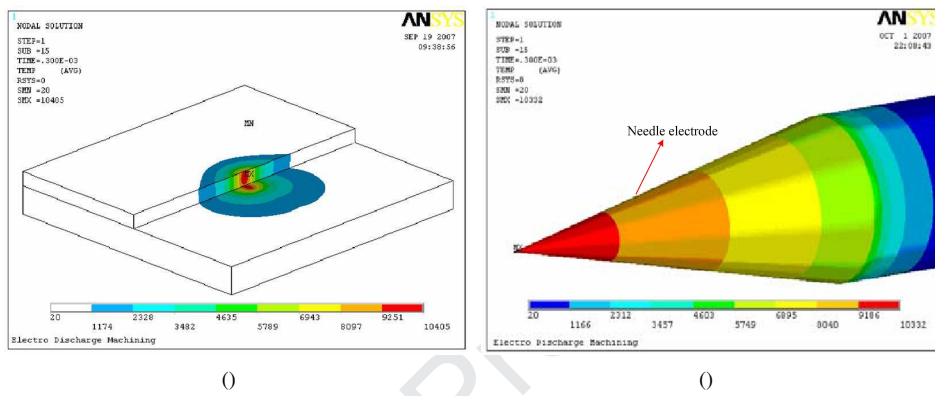


Figure 9: Temperature distribution for machining non-conductive advanced ceramic materials in EDM with assisted electrode ($U=20V$, $I=34A$, $Ton=300\mu s$); (a) auxiliary electrode and ceramic materials; (b) needle electrode [75].

Further, Liu et al. used the thin copper sheet, feeding the tool electrode, along the workpiece surface as the auxiliary electrode, and realized the EDM process of cutting advanced ceramics under water-based fluid [76]. Moreover, Gauss distribution of heat flux [72] was used to establish the removal model of non-conductive alumina-based ceramics by single pulse discharge. Hence, the thermal erosion characteristics of machining this ceramics were numerically simulated under single pulse discharge. By verifying the evaluation index of material removal volume, the error between the experiment and simulation was within 20% (in Fig.10). This is because that the removal mechanism of alumina-base advanced ceramics is the result of melting, evaporation and thermal spalling, and the efficiency of thermal spalling is higher than that of melting and evaporation. Therefore, it is difficult to take the effect of thermal spalling into account when the single pulse discharge model for machining non-conductive Al_2O_3 ceramics in EDM.

Based on finite element method (FEM) and finite volume method (FVM), Singh et al. [77] proposed a 2D axis-symmetric numerical model of WEDM-assisting electrode (AE) for insulating Al_2O_3 ceramics to analyze the effect of AE thickness on material removal mechanism. Combining simulation and experimental results, Figure 11 illustrated the relationship between AE thickness and MRR & Ra. MRR increased with the increase of AE thickness and turned to decrease after the critical point, while Ra kept decreasing with the increase of AE thickness all the time. This was because an increasing thickness of assisting electrode led to higher heat dissipation rate along the radial direction than that of vertical depth direction.

Mahdavinejad et al. [78] conducted a numerical study on instability in ED machining of silicon carbide (SiC) due to heat transfer in the workpiece substrates. This thermal process was significantly affected by plasma channel and heat transfer behavior in the workpiece body. A cylindrical coordinate model had been meshed in radial, vertical and surrounding direction using finite difference method (FDM) to solve the differential equations of heat transfer and electrical potential in the workpiece body. The results revealed that high voltage reduction resulted in a waste of energy regarding as Joule heating, which reached maximum on the surface of SiC workpiece for short pulse durations and near the surface in depth for long pulse durations. The temperature gradient of workpiece sharply decreased along depth and surface directions.

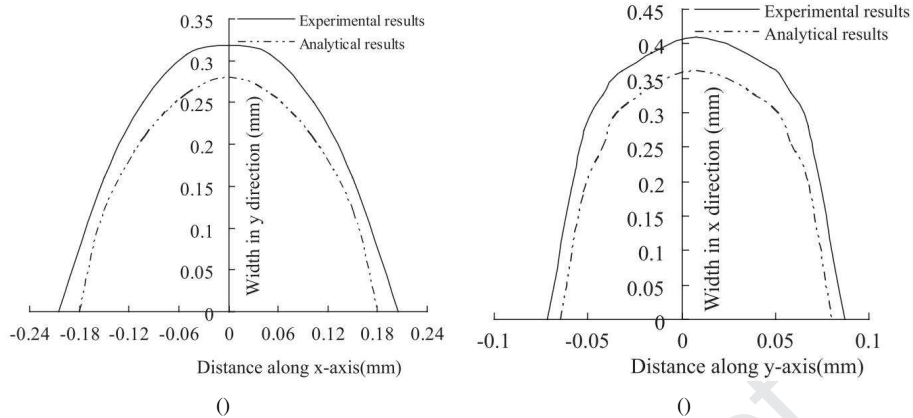


Figure 10: Crater sizes due to single-pulse for EDM insulating Al_2O_3 ceramics and its verification; (a) variation of width in the y direction for removal materials; (b) variation of width in the x direction for removal materials [76].

3.1.2. Conductive ceramics

Fukuzawa et al. [79] investigated residual stress levels and distributions of TiB_2 -base ceramic reshaped by EDM with a nickel electrode using a 2D FEM based on an elasto-plastic condition. It was found that crack propagation behavior was closely related to residual stress distribution. Saxena et al.[80] propose a coupled thermo-structural process model to evaluate Micro-EDM characteristics of conductive SiC ceramic. This FE model used a Gaussian heat flux distribution to predict the transient temperature distribution in heating phase, as well as crater dimensions, volume of material removed, and thermal residual stresses in cooling phase under different process parameters and material properties. The preliminary experiments were carried out to validate this model which still existed some defects due to its limitation in estimation of spark point distribution and secondary discharge effect.

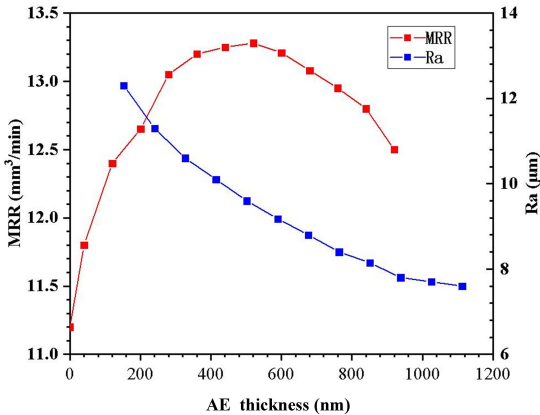


Figure 11: Variation of MRR and Ra with AE thickness [77].

For multi-phase ceramics, the thermal-physical and mechanical properties of each phase are quite different. In the process EDM, the heat transfer of the multi-phase materials is not uniform. Due to the different melting points of each phase, the phenomenon of variant erosion may occur, which affects the machining quality of the machined material surface. Ma established the single pulse discharge model for ZrB_2 -SiC, and realized the random distribution of SiC particles in ZrB_2 matrix by programming with APDL language in ANSYS, as shown in Figs.12a-c [81]. In the simulation model of ZrB_2 -SiC, Gauss distribution of heat flux was also used in the heat source of FEM. As shown in

Fig.12d, the simulation results showed that there were pits on the etched contour due to the different melting points of ZrB₂ and SiC. In addition, the radius and depth of the crater were increase of pulse-on time. By conformation experiments, the simulation value of the crater radius was slightly less than the experimental value. The average deviation between the numerical and experimental values was 3.62μm (with 12.48% average error) [81].

To improve the MRR, a technique of USEDM of metal matrix composites was proposed by Pupaza [82]. Considering the ultrasonic effect, the thermal shock phenomenon and its influence on the material removal process were analyzed by the finite element method. The results showed that the temperature of Al₂O₃ particles did not reach its melting temperature though the melting temperature of the matrix material is exceeded, and large internal stress was produced in the material because of the non-uniformity of heat flow distribution, which led to the spalling phenomenon during EDM process of the material [82].

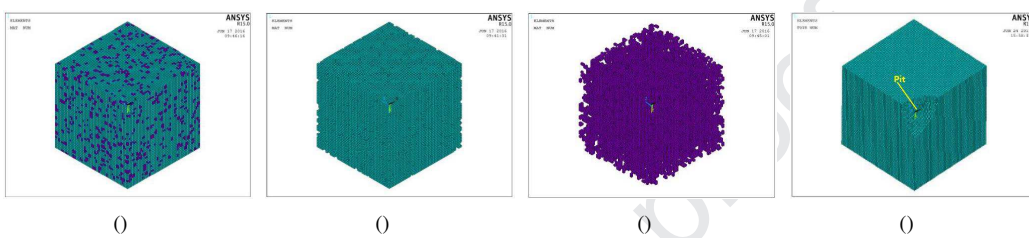


Figure 12: Mesh and simulation results of ZrB₂-SiC advanced ceramics; (a) ZrB₂-SiC advanced ceramics; (b) ZrB₂ matrix; (c) SiC reinforcement; (d) simulation results (U=20V, I=13A, Ton=20μs) [81].

3.1.3. Summary

To sum up, finite element method (FEM), finite volume method (FVM), and finite difference method (FDM) were most popular modeling approaches, implemented to establish thermo-physical model of ED machining advanced ceramics. Table 4 listed the lasted researches on modeling the EDM process of ceramics. FE model could not only predict transient temperature distribution [75, 76, 80] and crater dimensions [76, 80, 81], but also numerically analyze residual stress distribution [79, 80, 83], deformation [83], micro structure, and machining performance like MRR, TWR, Ra [76, 84]. FV model could also simulate the temperature field [85] and machining characteristics [77] even in micro scale material removal process of micro-EDM. FD model could simulate plasma channel [78], heat transfer[78, 86, 87], melting zone [78, 88], crater morphology and MRR [88] in the EDM process. By comparison, FEM and FVM were widely used in modeling thermo-physical process of EDM including transient temperature distribution, material transformation, material removal, and crater formation. Because FEM and FVM do well in multi-physics coupling simulation and complexity adaptability of computational domain, which better to accord with the complexity of practical ED machining ceramics.

Assisting electrode technique is important to EDM process of non-conductive ceramics, and heat transfer characteristics and thickness of assisting electrode layer significantly affected machining performance of EDM. Since MRR increased with the increase of AE thickness and turned to decrease after the critical point [77], appropriate thickness of AE was critical to achieve desired MRR. Tahmasebipour et al. [85] found central temperature of workpiece could be increased by 80% when 50nm Au film was selected as AE for nano-EDM process of Si according to numerical simulation results. Thus, through combining numerical and experimental researches, the effect of thickness, material properties and process parameters on machining performance of ED machining ceramics, like MRR, Ra, TWR, could be revealed.

Table 4: Comparisons of modeling advancements in electric discharge machining

method	Author	Contributions	Research objectives
FEM	Yu et al.[75]	A single pulse discharge model for EDM with assisted electrode of non-conductive advanced ceramics	Transient temperature distribution
	Saxena et al. [80]	Evaluate the characteristics of conductive SiC processed by μ EDM based on a coupled thermo-structural model	Transient temperature distribution, Crater dimensions, Volume of material removed, Thermal residual stresses
	Liu et al. [76]	Numerical analysis on thermal erosion characteristics of ED milling insulating Al_2O_3 ceramic with single pulse discharge	Three-dimensional temperature fields, Spalled ceramic surface.
	Fukuzawa et al. [79]	Study on crackpropagationbehavior of TiB_2 -baseceramicreshaped by EDM using a 2D FEM	Residualstress distribution
	Das et al. [83]	A finite element-based model for EDM process to predict transient temperature distribution, material transformation, and crater shape	Deformation, Microstructure, Residual stresses
	Marafona et al. [84]	A finite element model of EDM based on the Joule effect	MRR, TWR, Surface roughness
FVM	Ma et al. [81]	A single pulse discharge model for $\text{ZrB}_2\text{-SiC}$	Crater radius
	Tahmasebipour et al.[85]	A heat transfer model of Nano EDM process using finite volume based CFD method	Temperature distribution
FDM	Singh et al. [77]	A 2D axis-symmetric model of WEDMC assisting electrode using Finite element and Finite volume method	Material removal characteristics
	Mahdavinejad et al. [78]	Numerical analysis on heat transfer in EDM process of SiC	Plasma channel radius, Temperature distribution, Melting zone
Banerjee et al. [86]	Numerical evaluation of transient thermal loads on wire electrode of WEDM under multiple discharge condition, the random pulse model for thin workpiece and the clusters model for thicker workpieces	Transient temperature distribution	

Izquierdo et al. [87]	A numerical model of the EDM process considering the effect of multiple discharges	Temperature fields
Tlili et al. [88]	An improved numerical model considering the growth of the plasma channel and the instantaneous removal of material	MRR, Morphology of the crater

3.2. Removal mechanism

Compared with machining metal materials, EDM of advanced ceramics has some different characteristics. Because of their high melting point, it needs higher discharge energy to melt and evaporate these materials. In addition, material removal caused by thermal stress is more likely to occur in EDM of advanced ceramics. Due to the limitation of resistance of advanced ceramics, the selection of parameters of pulse power is also limited in the process of EDM. When machining metal materials, for the pulse width less than $1\mu\text{s}$, the main removal mechanism of EDM was electromagnetic force and electrostatic force. However, in a long pulse width, melting, evaporation and thermal spalling are the main reasons for its removal [89]. Whether the material removal was melting, evaporation or thermal spalling largely depended on the process parameters of EDM and the physical and mechanical properties of the machined materials [89, 90].

According to Lee et al., the removal mechanism of ED machining Al_2O_3 -TiC was attributed to melting, evaporation, oxidation, and thermal spalling. In addition, compared with the usual melting and evaporation, the thermal micro-cracks in the ceramic workpiece caused high removal volume, resulting in high surface roughness (in Fig.13) [89]. For the non-conductive ceramic EDM, the material removal mechanism was mainly attributed to the thermal spalling caused by the alternating heat load during the pulse-on and pulse-off times of EDM [89]. Therefore, the discharge energy had a great influence on material removal [90, 91, 92].

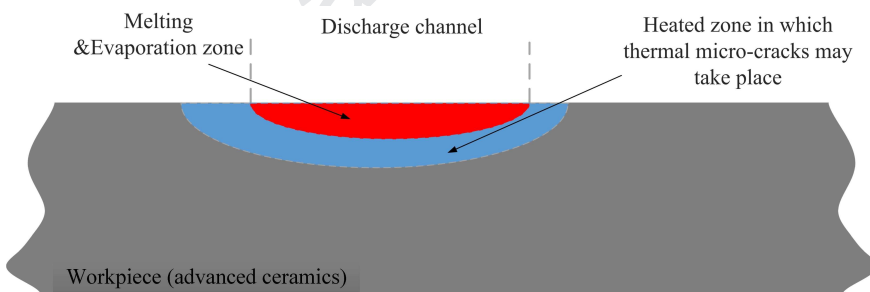


Figure 13: The effect of thermal spalling when cutting advanced ceramics [89].

To investigate the material removal mechanism of conductive ceramics in the process of WEDM, Lauwers et al. analyzed ceramic debris and surface/sub surface quality of ZrO_2 -based, Si_3N_4 -based and Al_2O_3 -based ceramic materials [91]. In their study, three types of material removal mechanism (melting/evaporation, thermal spalling and oxidation/decomposition) were suggested in the process of WEDM for these different advanced ceramics. Their research on WEDM of zirconia ceramics showed that the material removal mechanism of melting/evaporation may occur due to the presence of multiple droplets on the machined surface as shown in Fig.14a. In addition, micro-cracks on the recast layer were found in the cross section of the machined surface. When the high energy condition was used in the process of EDM, this kind of material removal mechanism (thermal spalling) could be observed in cutting Al_2O_3 -SiCW-TiC. As depicted in Fig.14b, larger micro-cracks were occurred in the regimes under high energy condition. In addition, the WEDM Si_3N_4 -TiN also showed similar thermal spalling mechanism. The irregular shape of the debris produced in this process included round and sharp edges, which further confirmed the thermal spalling mechanism. On the other hand, foam and porous layers appeared in cutting Si_3N_4 -TiN material in the process of WEDM, as shown in Fig.14c. The foam microstructures were caused by the formation of gas bubbles. This was

attributed to the visual appearance of bubbles and the smell of ammonia in the experiments. The thermal energy, generated by the process of WEDM, contributed to the oxidation /decomposition of the advanced ceramics, which eventually led to these effects.

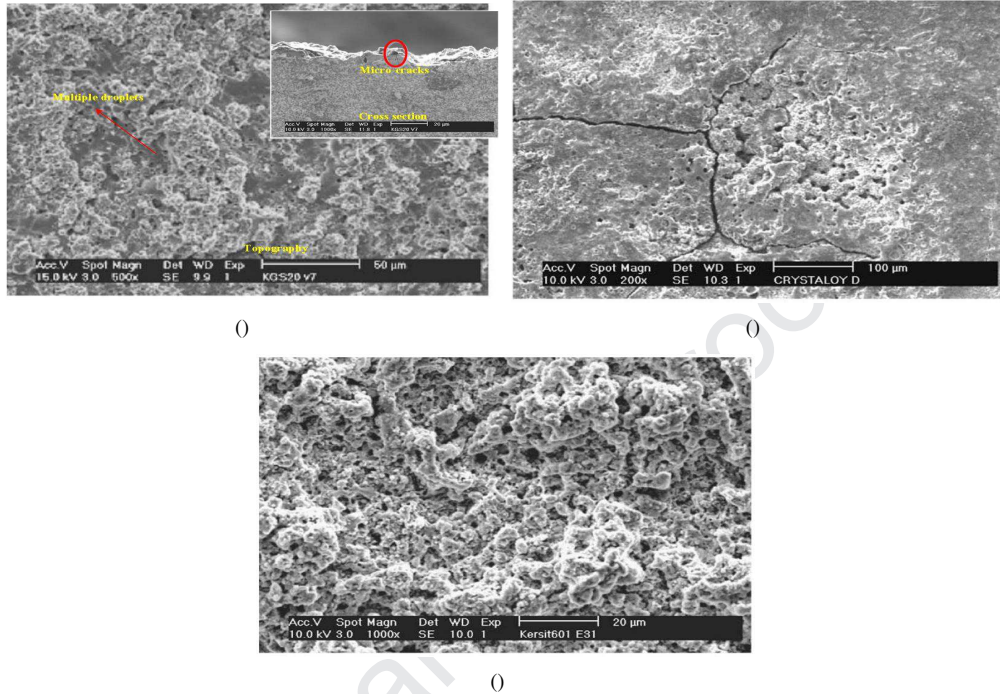


Figure 14: The SEM of three types of material removal mechanism; (a) SEM of ZrO₂CTiN by wire EDM ($U = 120$ V, $T_{on} = 2.4\mu s$, $T_{off} = 15\mu s$); (b) SEM of Al₂O₃-SiCW-TiC by wire EDM ($U = 250$ V, $T_{on} = 7.5\mu s$, $T_{off} = 18\mu s$); (c) SEM of Si₃N₄CTiN by wire EDM ($U = 160$ V, $T_{on} = 2.8\mu s$, $T_{off} = 2.3\mu s$) [91].

Adding MWCNTs to zirconia ceramics can significantly improve its conductivity, which makes the composites directly processed by EDM. Melk et al. studied the surface integrity of composites with 1% and 2% MWCNTs after EDM, and showed that the material removal mechanism of the two composites was melting/evaporation and thermal spalling [93]. As depicted in Fig.15a, there were many droplets in clusters in the two composites. In Fig.15b, a recast layer with micro-cracks was shown on the EDM surface. These cracks probably were related to thermal shock because of the low thermal conductivity of the two composites. In addition, this phenomenon was also related to the thermal expansion difference between the recast layer and the matrix of the two composites during the cooling process. As shown in Figs.15c-d, a recast layer with a thickness of several micrometers was formed on the machined surface, and the presence of ZrC can be detected by XRD. Furthermore, Raman spectroscopy showed that some MWCNTs survived although there was a high temperature by EDM.

4. Machining performance indicators

It is well known that the machining performance indicators are affected by electrical parameters and non-electrical parameters in the process of EDM. For cutting advanced ceramic materials, however, workpiece and tool electrode materials had a significant impact on the machining performance indicators, which was significantly different from that of cutting metal materials[94]. Hence, the effects of workpiece and tool electrode were described independently from non-electrical parameters, and Fig.16 illustrated the fishbone diagram of machining performance indicators of advanced ceramic materials by EDM.

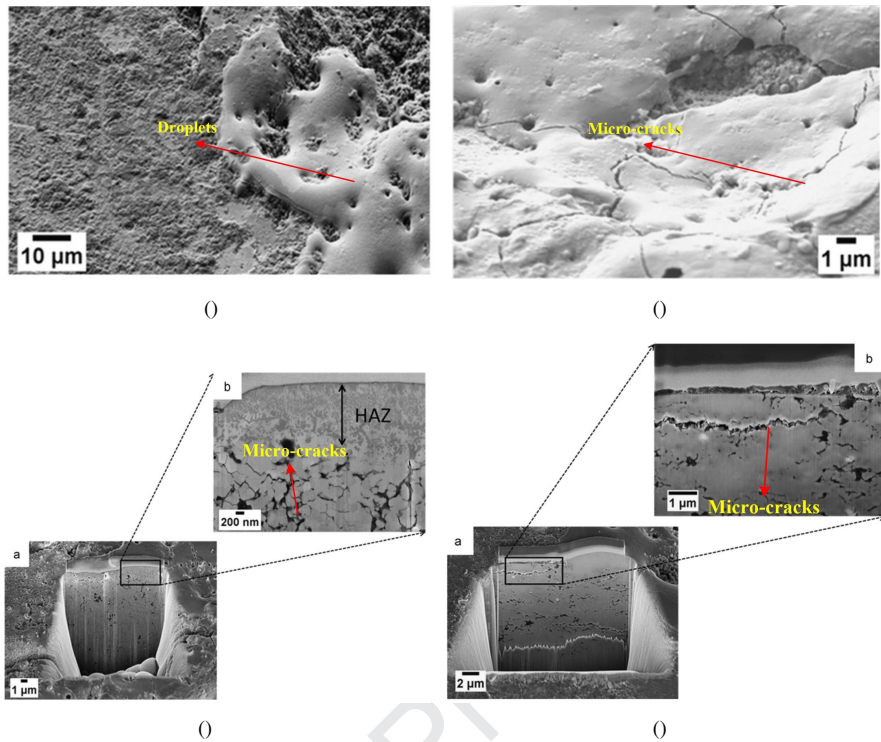


Figure 15: The SEM of three types of material removal mechanism ($U = 205$ V, $I=3.2$ A, $T_{on} = 2.1\mu s$, $T_{off} = 4.9\mu s$); (a) Melting/evaporation in composite with 1 wt% CNT content; (b) Melting/evaporation in composite with 2 wt% CNT content; (c) the recast layer of the composite with 1 wt% CNT content; (d) the recast layer of the composite with 2 wt% CNT content [93].

According to the electrical conductivity of advanced ceramics, the reviews of MRR, surface roughness, TWR, and surface topography and micro-structures were divided the basic of machining advanced ceramics into two approaches, which were EDM-assisting electrode used for non-conductive ceramics and common EDM process of conductive ceramics like ceramic composites. Moreover, the specific discharge energy (SDE) was introduced into this section to comprehensively review the latest researches of MRR.

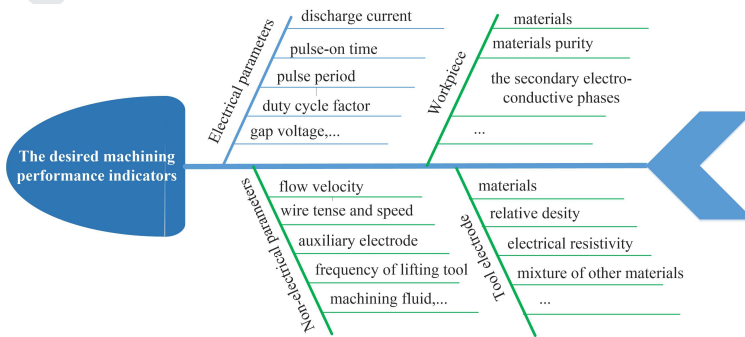


Figure 16: Fishbone diagram of machining performance indicators of advanced ceramic materials by EDM

4.1. MRR

4.1.1. Non-conductive ceramics

Hanaoka et al. fabricated several silicon nitrides (Si_3N_4) ceramics with carbon nanostructure composite materials and machined using the assisted electrode technique in the process of EDM [17]. For different materials cut by EDM, the MRR value decreased with the increase of electrical conductivity, and the value of without assisted electrode was smaller than that of with assisted electrode. The maximal MRR that can be obtained with discharge current=5A, pulse-on time=1.0 μs , and electrical conductivity=1E-13 was 0.25 mm³/min.

Fukuzawa et al. studied the EDM process of Al_2O_3 ceramics using assisted electrode technique [95]. It was found that with the increase of alumina purity, the MRR decreased and the processing tended to be unstable. The maximal MRR (0.04mm³/min) was obtained during the EDM process of 92% Al_2O_3 ceramics with discharge current=1A, pulse-on time=1.0 μs , pulse period =64 μs and gap voltage =320V. This was because that the adhesion of the conductive layer was related to the thermal conductivity, thus affecting the stability of the discharge (listed in Fig.17). Liu et al. studied the influence of tool polarity, gap voltage, rotation speed and workpiece feed speed on MRR during ED-milling of Al_2O_3 ceramic using thin copper as assisted electrode [96]. The high MRR required positive processing and large pulse duration. The effects of different concentrations of machining fluids on MRR were also studied. The results showed that water-based emulsion had the better discharge waveform (depicted in Fig.18).

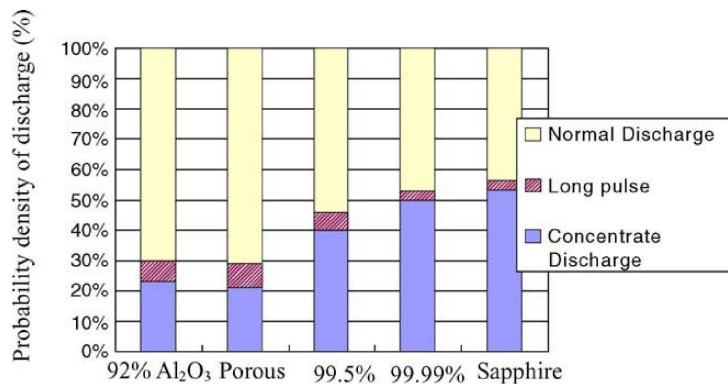


Figure 17: Distribution of discharge waveform of machining Al_2O_3 ceramics by EDM [95].

Sabur et al. investigated the effect of discharge energy on MRR during EDM of non-conductive ZrO_2 , and discussed the mechanism of material removal. The mechanism of material removal was mainly through thermal spalling, and MRR increased with the increase of discharge energy [29]. The maximal MRR was obtained at 0.24 mm³/min when the discharge current = 6A , pulse-on time = 12 μs , and pulse period =24 μs . By use of the assisted electrode method, Fukuzawa et al. studied the EDM of ZrO_2 with porous copper electrode [97]. The practical duty factor for each relative density of the porous tool electrode was listed in Fig.19. The results showed that the desired machining performances could be acquired when the relative density of cathode was 85%. Therefore, the maximal MRR was obtained at 0.32 mm³/min when the discharge current, pulse-on time, and pulse period were 4.67A, 16 μs and 64 μs , respectively.

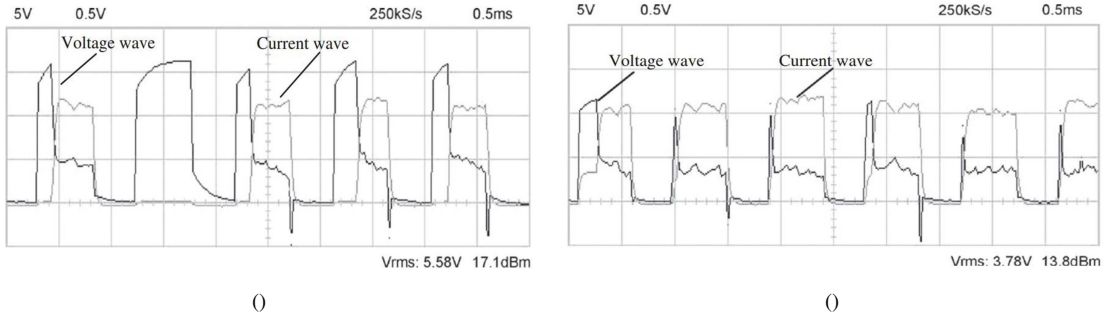


Figure 18: Discharge waveform of machining Al_2O_3 ceramics by ED-milling in different machining fluids; (a) with 5% emulsion+water; (b) with 5% emulsion+0.5% NaNO_3 +water [96].

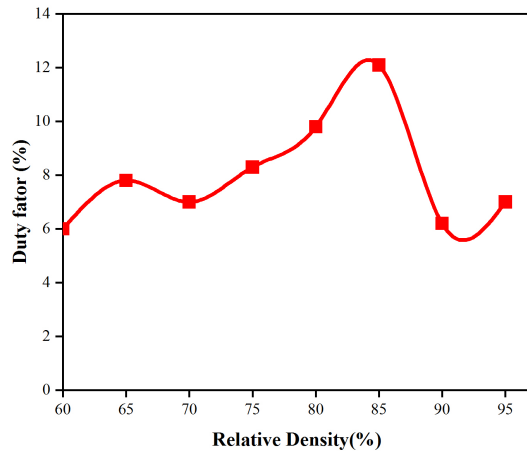


Figure 19: Practical duty factor for each relative density of the porous tool electrode [97].

4.1.2. Conductive ceramics

Puertas et al. investigated a study of optimization of machining parameters for cutting boron carbide (B_4C) by EDM, and they found that the MRR varied from 0.135 to $0.396 \text{ mm}^3/\text{min}$ under the discharge current $3\text{-}5\text{A}$, pulse period $10\text{-}50\mu\text{s}$, and duty cycle factor $0.4\text{-}0.6$ [98]. It could be concluded that the duty cycle factor seriously affects MRR, and the subsequent process parameters were discharge current and pulse period, respectively. When the duty cycle factor increases, the MRR tended to increase. Moreover, Puertas et al. investigated the influence of discharge current, pulse-on time, duty cycle factor, gap voltage and dielectric flushing pressure on the MRR in the EDM process of B_4C [99]. The second-order model for MRR was selected to build the relationship between these cutting process parameters and MRR, and R^2 and R_{adj}^2 of the model were 0.978 and 0.960 , respectively. The experimental results showed that MRR increased with the increase of discharge current and pulse-on time, which was consistent with the machining of metal materials, because high-energy pulse would lead to a higher MRR. The maximal MRR was obtained at $0.740 \text{ mm}^3/\text{min}$ when the discharge current was 6A and pulse-on time was $30\mu\text{s}$.

Clijsters et al. developed a kind of EDM technique in commercial silicon carbide (Si-SiC), and studied the influence of main process parameters on the MRR [15]. They found that the mechanism of material remove was mainly considered as melting and evaporation, similar to the EDM of steel, and that the significant parameter for the MRR

was the process parameters of gap voltage. When the maximum gap voltage of 200V was applied, it was noted that the optimum discharge current of 32A provides the maximum material removal of $6.01\text{mm}^3/\text{min}$. While the discharge current exceeded 32A, however, the MRR deceased. This was because that there was an optimal pulse-on time under a particular discharge current to yield an optimal MRR for the process of EDM. These optimal values were considered to be related to the corrosion resistance of the material, which may explain the decrease of MRR when discharge current was further increased [100]. Malek et al. studied the feasibility of using MWCNTs as the second phase of conducting to process Si_3N_4 , and carried out experiments with $\text{Si}_3\text{N}_4+5.3\text{vol}\%$ MWCNTs composite [18]. The results showed that the MRR of MWCNTs increased with the voltage until reaching 140V, and decreased slightly with the further increase of discharge energy. The maximum value of MRR was $1.27\text{mm}^3/\text{min}$, when the discharge current was 0.5A, gap voltage was 140 V, pulse period time was $2\mu\text{s}$, and pulse-on time was 20ns.

By adding conductive particles, non-conductive advanced ceramics materials can also become conductive materials. To obtain multi-objective characteristics, Patel et al. optimized the process parameters in EDM of Al_2O_3 ceramic composite ($\text{Al}_2\text{O}_3\text{-SiC}_w\text{-TiC}$) under grey relational analysis method [101]. It could be found that the discharge current was the most significant factor that affects the MRR. The maximal MRR was $1.08\text{ mm}^3/\text{min}$, when the discharge current, pulse-on time, duty cycle factor, and gap voltage were 7A, $150\mu\text{s}$, 0.64, and 50V, respectively. Bonny et al. studied the effect of secondary electro-conductive phases (with 40 vol.% WC, TiCN or TiN) on the EDM of ZrO_2 ceramic composites [102]. The removal mechanism was full melting and evaporation in the process of EDM. As depicted in Fig.20, the maximal MRR of $33.54\text{ mm}^2/\text{min}$ could be gained for the $\text{ZrO}_2\text{-WC}$ when the discharge current, pulse-on time, and pulse period were 350A, $2.4\mu\text{s}$, and $20\mu\text{s}$, respectively.

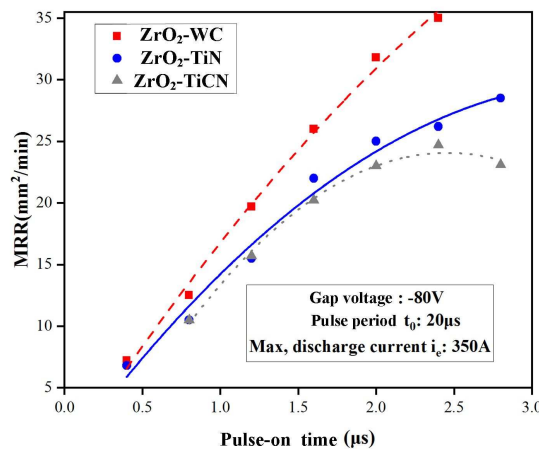


Figure 20: Relationship between MRR and pulse-on time (pulse duration) when machining ZrO_2 advanced ceramic composites with different secondary electro-conductive phases [102].

4.1.3. Summary and SDE analysis

In summary, Table 5 listed the summary of MRR for EDM process of advanced ceramics (non-conductive ceramics and conductive ceramics). It could be drawn from Table 5 that the discharge energy was the dominated role of MRR. High MRR could be acquired under high values of discharge current, pulse-on time, gap voltage, and duty cycle factor. This phenomenon was similar to cutting metal materials by EDM. Because the thermal conductivity of advanced ceramic materials was lower than that of metals in general, however, the discharge energy should not be too high. Compared with cutting metal materials, low discharge current and short pulse-on time were applied in machining advanced ceramics [17, 18, 29, 95, 96, 98, 99]. Due to the high melting point and brittleness of them, the machining efficiency is generally lower than that of metal materials to maintain the machining accuracy. In addition, electrical conductivity, material purity, the secondary electro-conductive phases, relative density of tool electrode,

and machining fluid were the important factors that affected the MRR. As mentioned above, the MRR decreased with increase of both the electrical conductivity [17] and alumina purity [95]. Among Zr-based advanced ceramics, ZrO_2 -WC exhibited better machinability in EDM [102]. As for the effect of the relative density of tool electrode on machining ZrO_2 , the desired machining performances could be acquired when the relative density was 85% in the process of assisted electrode EDM [97].

To illustrate the relationship between the machining performance of materials and its property, Liao [103] proposed the concept of SDE in wire-EDM. By this method, a quantitative method was put forward to estimate the energy efficiency in the process of EDM. It could be concluded that there was a low MRR in the process of EDM, compared with traditional machining method. Therefore, the comparison of SDE in machining advanced ceramics was listed in Fig.21. On the whole, the SDE distribution range was 0.3-28kJ/mm³ in the process of electric discharge machining advanced ceramics. While discharge current was 6A, the average values of SDE of machining Al6061, Inconel 718, and SDK11 were 0.52, 1.03, 0.98kJ/mm³, respectively [104]. Hence, the SDE in machining advanced ceramics was larger than that in machining metal materials. This phenomenon was that the melting point of advanced ceramics was much higher than that of metal materials; and the effect of heat was the main reason for material removal mechanism. It could be concluded from Fig.21 that the SDE of machining B_4C and ZrO_2 was higher than that of machining of others. In the process of machining Si_3N_4 , the SDE could be decreased by adding the second phase (5.3vol% CNTs) [17, 18]. The second phase CNTs not only enhanced the toughness of the material, but also improved the machining performances, such as energy efficiency. It could be also concluded that the SDE was related to discharge energy, and the SDE decreased with the increase of discharge energy in the process of machining B_4C [98, 99]. This phenomenon was also similar to our previous studies, in which the average SDE of all three materials (Al 6061, Inconel 718, and SDK11) was decreased with the increase of discharge energy [104].

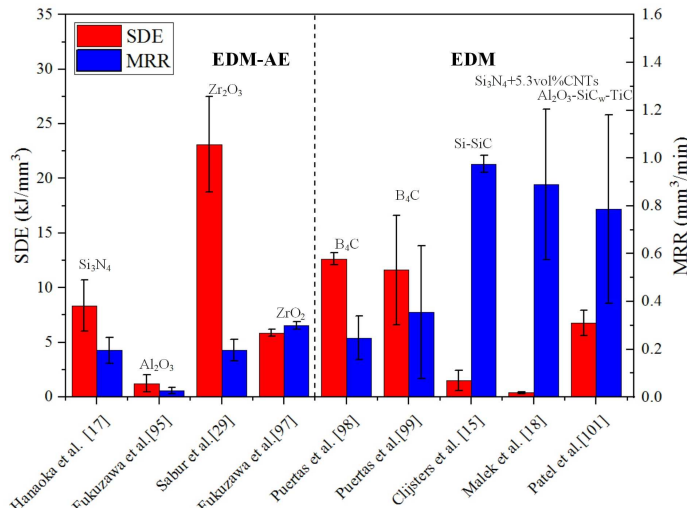


Figure 21: Comparison of SDE in machining advanced ceramics.

Table 5: Summary of MRR for EDM process of advanced ceramics

Machining method	Ceramics type	Process parameters	MRR	Remarks
EDM-AE	Si_3N_4 -CNTs	Si-based ceramics Discharge current, pulse-on time, and electrical conductivity.	Maximal value with $0.25 \text{ mm}^3/\text{min}$	The MRR value decreased with the increased of electrical conductivity [17].
	Al_2O_3	Al-based ceramics Discharge current, gap voltage, pulse-on time, pulse period, and material purity.	Maximal value with $0.04 \text{ mm}^3/\text{min}$	The MRR decreased with the increase of alumina purity [95].
	ZrO_2	Zr-based ceramics Discharge current, pulse-on time, pulse period, and the relative density of tool electrode.	Maximal value with $0.24 \text{ mm}^3/\text{min}$	MRR increased with the increase of discharge energy [29].
EDM	B_4C	C-based ceramics Discharge current, pulse period, and duty cycle factor	$0.135-0.396 \text{ mm}^3/\text{min}$	The second-order model for MRR was built, and the response surface for it was estimated [98].
	$\text{Si}-\text{SiC}$	C-based ceramics Discharge current, pulse-on time, duty cycle factor, gap voltage and dielectric flushing pressure	Maximal value with $0.74 \text{ mm}^3/\text{min}$	High MRR can be acquired under high values of gap voltage, pulse-on time, and duty cycle factor [99].
EDM	Si_3N_4 -MWCNTs	Si-based ceramics Discharge current, gap voltage, pulse-on time, and pulse period.	Maximal value with $6.01 \text{ mm}^3/\text{min}$	The optimum discharge current was 32A for the desired MRR [15].
	Al_2O_3 -SiC _w -TiC	Al-based ceramics Discharge current, pulse-on time, duty cycle factor, and gap voltage.	Maximal value with $1.27 \text{ mm}^3/\text{min}$	The optimum gap voltage was 140V for the desired MRR when cutting $\text{Si}_3\text{N}_4+5.3\text{vol\% MWCNTs}$ composite [18].
				The discharge current was the most significant factor that affects the MRR [101].

ZrO ₂ -WC	Zr-based ceramics	Discharge current, pulse-on time, pulse period, and the secondary electro-conductive phases.	Maximal value with 0.31mm ³ /min	ZrO ₂ – WC exhibited better performance in EDM machinability of MRR [102].
ZrO ₂ -TiN				
ZrO ₂ -TiCN				

4.2. Surface roughness

4.2.1. Non-conductive ceramics

Using the assisted electrode technique, Hanaoka et al. also investigated the surface roughness of machining the several silicon nitrides (Si_3N_4) ceramics with carbon nanostructure composite materials in the process of EDM [17]. The experimental results showed that the Ra value decreased with the increase of electrical conductivity, and the rougher surfaces were observed on the assisting electrode method. As depicted in Fig.22, surface roughness (Ra) was as a function of the electrical conductivity. The minimal Ra can be acquired with discharge current=5A, pulse-on time=1.04μs, and electrical conductivity=1E+4 was 1.2μm.

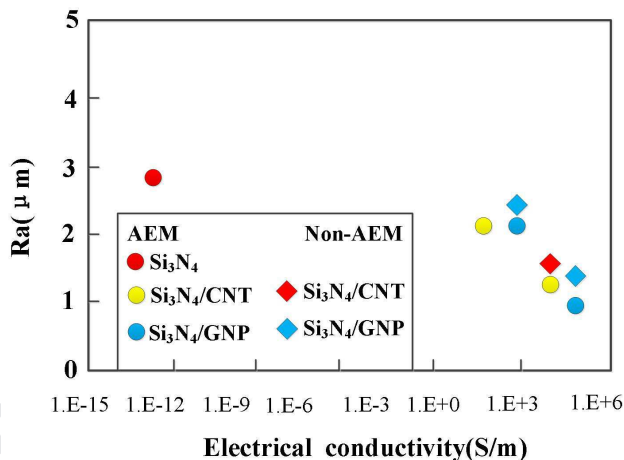


Figure 22: Surface roughness (Ra) was as a function of the electrical conductivity[17]

Fukuzawa et al. explored the surface roughness of cutting ZrO₂ with porous copper electrode in EDM [97]. The results showed that the values of Ra were achieved within the error range of each relative density while the MRR increased. This was because that the height and diameter of discharge craters were related to the surface roughness under the same cutting conditions, which depended on the physical properties of electrode materials, including thermal conductivity, melting point, and gasifying temperature.

To machine insulating ceramics (Al_2O_3), Fukuzawa et al. adopted a PVD-TiN layer as the assisting electrode [95]. Fig.23 depicted the relationship between surface roughness (Ry) and thermal conductivity for machining Al_2O_3 . The surface roughness (Ry) increased with increase in thermal conductivity (λ), which correlated to material purity except for porous materials [97]. The minimal surface roughness (Ry) (29μm) was obtained during the EDM process of 92% Al_2O_3 ceramics with discharge current=1A, pulse-on time=1.0μs, pulse period =64μs and gap voltage =320V.

Liu et al. investigated effects of different concentrations of dielectrics (emulsion, NaNO_3 and polyvinyl alcohol) on the Ra [96]. The results showed that the size of crater produced by single pulse with 0.5% polyvinyl alcohol (PVA) concentration was larger than that without PVA. Therefore, the Ra increased with the increase of PVA concentration.

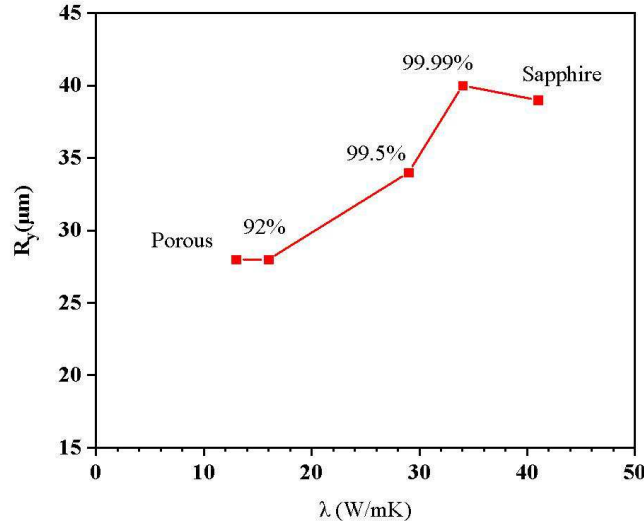


Figure 23: Relationship between surface roughness (R_y) and thermal conductivity for machining Al_2O_3 ceramics[95]

4.2.2. Conductive ceramics

In Puertass study, the Ra for electric discharge machining boron carbide was also investigated. The experimental results showed that the surface roughness (Ra) varied from 1.30 to $2.27\mu\text{m}$ under the discharge current $3\text{-}5\text{A}$, pulse period $10\text{-}50\mu\text{s}$, and duty cycle factor $0.4\text{-}0.6$ [98]. It could be also concluded that the pulse period seriously affected the surface roughness (Ra), and the subsequent process parameters are discharge current and pulse period, respectively. The Ra turned to be worse with the pulse period increasing, while the Ra came to decline with the increase of discharge current or duty cycle factor. In addition, Puertas et al. investigated the influence of discharge current, pulse-on time, duty cycle factor, gap voltage and dielectric flushing pressure on Ra when machining B_4C in the process of EDM [99]. The second-order model for Ra was selected to build the relationship between these process parameters and MRR, and R^2 and R_{adj}^2 of the model were 0.978 and 0.954 , respectively. The experimental results showed that the estimated response surface of Ra was a function of strength and voltage, and that Ra decreased with the increase of discharge voltage, which was not consistent with the general practice of metal materials. This phenomenon was that the conductivity of ceramic materials was lower than that of metal materials. The minimal Ra of $1.82\mu\text{m}$ was obtained while the discharge current, pulse-on time, open voltage and duty cycle factor were 3A , $30\mu\text{s}$, 200V and 0.6 , respectively.

Clijsters et al. investigated the effect of key process parameters on Ra while machining Si-SiC [15]. They found that the significant parameters for Ra was the discharge current and gap voltage. Using the proposed machining strategy in finishing stage, the minimal surface roughness Ra of $1.05\mu\text{m}$ could be obtained while discharge current, pulse-on time, gap voltage, and pulse period were 6A , $6\mu\text{s}$, 200V , and $25\mu\text{s}$, respectively. In addition, the relationship of MRR and surface roughness Ra of each experiment was built, which was depicted in Fig.24. The desired Ra was obtained at the expense of decreasing MRR, which was similar to that in machining metal materials in EDM. Malek et al. compared the machining performance of $\text{Si}_3\text{N}_4/\text{MWCNTs}$ and $\text{Si}_3\text{N}_4/\text{TiN}$ in the process of EDM [18]. The results showed that the machining performances of both Ra and MRR of $\text{Si}_3\text{N}_4/\text{MWCNTs}$ were better than that of $\text{Si}_3\text{N}_4/\text{TiN}$ while the process parameters were same, which was depicted in Fig.25. In addition, the surface roughness Ra increased while the high MRR was desired. The surface of $\text{Si}_3\text{N}_4/\text{MWCNTs}$ was very smooth, and the minimum Ra value was $0.21\mu\text{m}$, which was almost independent of the gap voltage. However, the Ra value of $\text{Si}_3\text{N}_4/\text{TiN}$ was four times higher than that of $\text{Si}_3\text{N}_4/\text{MWCNTs}$, and improved with the gap voltage increasing. Krishna et al. performed experimental studies the features of micro-ED machining conductive SiC [105]. Through the optimization experiment, the best machining conditions for obtaining good surface roughness were 150V , 0.1mF and 60% threshold in micro EDM of SiC advanced ceramics.

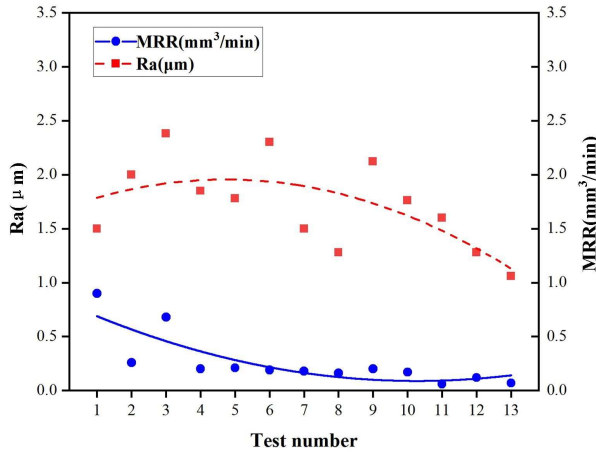


Figure 24: The relationship of MRR and Ra of each experiment on processing Si-SiC [15].

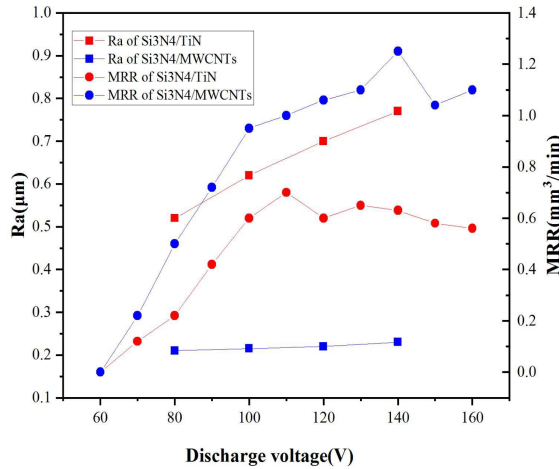


Figure 25: MRR and Ra are as a function of the discharge voltage, respectively [18].

For machining $\text{Al}_2\text{O}_3/\text{SiC}_w/\text{TiC}$, Patel et al. determined the optimal parameter combination based on the prediction model of surface roughness. They revealed that the Ra varied from 0.72 to $3.30\mu\text{m}$ under the discharge current $3\text{-}7\text{A}$, pulse-on time $10\text{-}200\mu\text{s}$, and duty cycle factor $0.24\text{-}0.88$ [106]. Moreover, it was also observed that the pulse-on time was the main parameter affecting surface roughness (Ra), and the increase of pulse-on time will increase it. However, the Ra turned to be worse under the increasing discharge current, and decreases gradually after reaching the peak value, shown in Fig.26.

Lee et al. found that better surface finish could be achieved if the positive electrode (workpiece) was used to machining $\text{Al}_2\text{O}_3/\text{TiC}$ [89]. The phenomenon was similar to that of machining metal materials in EDM. Also, the surface roughness increased with increase of the pulse-on time, and the minimum was $0.2\mu\text{m}$ under the low pulse-on time ($40\mu\text{s}$). To optimize the process parameters in EDM of Al_2O_3 ceramic composite ($\text{Al}_2\text{O}_3 - \text{SiC}_w\text{-TiC}$), Patel et al. found that the discharge current and duty cycle factor were the most significant factor for the grey relational grade, and that the pulse-on time and gap voltage had been also found to be significant[101]. The minimal Ra $3.39\mu\text{m}$, for multi-performance, could be obtained when the discharge current, pulse-on time, duty cycle factor, and gap voltage were 7A , $150\mu\text{s}$, 0.8 , and 50V , respectively.

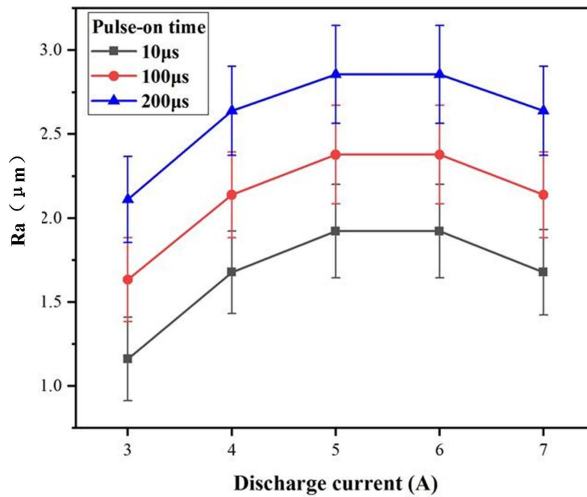


Figure 26: Ra varies with process parameters in EDM of $\text{Al}_2\text{O}_3/\text{SiC}_w/\text{TiC}$ ceramics [106].

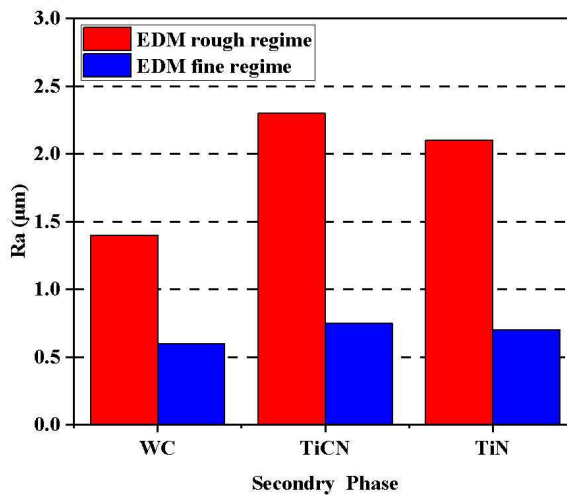


Figure 27: Surface roughness of ZrO_2 -based advanced ceramics under different secondary phase additions [102].

Bonny et al. investigated the influence of secondary electro-conductive phases on the surface roughness R_a of Zr -based advanced ceramics in EDM [102]. As shown in Fig.27, it could be concluded that ZrO_2 -WC of EDM exhibited better surface roughness in both rough and fine regime , and that the minimal R_a of rough regime and fine regime were 1.48 and 0.55 μm , respectively.

4.2.3. Summary

Similar to cutting metal materials, there was a conflict between the MRR and the surface roughness R_a while machining advanced ceramics by EDM [90, 92, 96, 106]. Table 6 listed the summary of EDM surface roughness R_a for advanced ceramics. The electric process parameters were significantly important to affect the Ra in the processes of both EDM-AE and EDM. However, the desired Ra was obtained at the expensive of MRR. This was because that the high discharge energy enhanced the size of craters, resulting in high MRR. Also, the surface roughness Ra was

increased due to large craters. Hence, the multi-objective optimization should be performed in the EDM of advanced ceramics. Compared the machining performance of $\text{Si}_3\text{N}_4/\text{MWCNTs}$ and $\text{Si}_3\text{N}_4/\text{TiN}$, the surface roughness Ra of the former was almost independent of the gap voltage [18]. The low surface roughness Ra could be acquired by applied the secondary phase WC [102]. In addition, the discharge status could be improved when the relative density of tool electrode varied and the same discharge conditions applied, resulting in good MRR [96]. Fortunately, the surface roughness was almost the same under this machining condition. To obtain the desired Ra , the high-priority strategy included selecting advanced materials, changing the materials purity, and adding the secondary electro-conductive phases.

Table 6: Summary of EDM machining performance surface roughness for advanced ceramics

Machining method	Ceramics type	Process parameters	MRR	Remarks
EDM-AE	Si_3N_4	Si-based ceramics Discharge current, pulse-on time, and gap voltage.	Minimal Ra with $1.2\mu\text{m}$	The surface roughness (Ra) value decreased with the increase of electrical conductivity [17].
	ZrO_2	Zr-based ceramics Discharge current, pulse-on time, pulse period, and the relative density of tool electrode.	$\text{Rz}:14-18\mu\text{m}$	The surface roughness was nearly the same when the relative density of tool electrode varied. [97].
	Al_2O_3	Al-based ceramics Discharge current, gap voltage, pulse-on time, pulse period, and material purity.	Minimal Ry with $29\mu\text{m}$	The relationship between surface roughness (Ry) and thermal conductivity was constructed [95].
B_4C	C-based ceramics	Discharge current, pulse period, and duty cycle factor	$\text{Ra}:1.30-2.27\mu\text{m}$	The second-order model for Ra was built, and the response surface for it was estimated [98].
		Discharge current, pulse-on time, duty cycle factor, gap voltage and dielectric flushing pressure	Minimal Ra with $1.82\mu\text{m}$	The surface roughness Ra decreased with the increase of discharge voltage [99].
EDM	Si-SiC	Discharge current, gap voltage, pulse-on time, and pulse period.	Minimal Ra with $1.05\mu\text{m}$	The optimum discharge current and gap voltage for the desired Ra were 6A and 200V, respectively [15].
	$\text{Si}_3\text{N}_4\text{-MWCNTs}$	Si-based ceramics Discharge current, gap voltage, pulse-on time, and pulse period	Minimal Ra with $0.21\mu\text{m}$	The surface roughness Ra was almost independent of the gap voltage [18].
	SiC	Gap voltage, Capacitance, and Threshold	\	The surface roughness Ra increased due to gap voltage [105].

$\text{Al}_2\text{O}_3/\text{SiC}_w/\text{TiC}$		Discharge current, pulse-on time, and duty cycle factor, and gap voltage.	Ra:0.72-3.30 μm	The developed models can predict Ra accurately within 95% confidence interval [106].
$\text{Al}_2\text{O}_3/\text{TiC}$	Al-based ceramics	Discharge current, pulse-on time, and pulse-off time.	Minimal Ra with 0.2 μm	Better surface finish can be obtained when the positive electrode (workpiece) was used [89].
$\text{Al}_2\text{O}_3-\text{SiC}_w-\text{TiC}$		Discharge current, pulse-on time, duty cycle factor, and gap voltage	Minimal Ra with 3.39 μm	The minimal Ra 3.39 μm for multi-performance can be obtained [101].
ZrO_2-WC ZrO_2-TiN ZrO_2-TiCN	Zr-based ceramics	Discharge current, pulse-on time, pulse period, and the secondary electro-conductive phases.	Minimal Ra with 0.55 μm for fine regime	$\text{ZrO}_2 - \text{WC}$ exhibited better surface roughness in both rough and fine regime in EDM [102].

4.3. TWR

4.3.1. Machining non-conductive ceramics

Fukuzawa et al. studied TWR of ZrO_2 in EDM with porous copper electrode [97]. As shown in Fig.28, the wear rate of the electrode changed with the change of relative density. The wear process of the electrode was investigated by observing the change of the edge shape of the cylinder angle with the SEM images. It could be concluded that the suitable TWR could be acquired when the relative density of tool electrode is 85%.

To investigate the relationship between the electrical conductivity of Si_3N_4 ($\text{Si}_3\text{N}_4/\text{CNP}$ and $\text{Si}_3\text{N}_4/\text{GNP}$) and the machining technique in EDM (EDM and EDM-AE), Hanaoka et al. found that the TWR of insulating materials was higher than that of other conductive materials, and found that it decreased with the increase of conductivity of materials [17]. The TWR was as a function of the electrical conductivity, which was depicted in Fig.29.

Moreover, the TWR increased with the increase of discharge energy during the EDM of non-conductive ceramics efficiently with high energy capacitor [107]. Ji et al. investigated the performance of high-energy capacitors on insulating ceramics by single discharge machining. The effect of process parameters on the TWR was shown in Fig.30 [107]. The TWR increased with an increase in both peak voltage and capacitance, but it decreased with an increase in both current-limiting resistor and tool electrode section area.

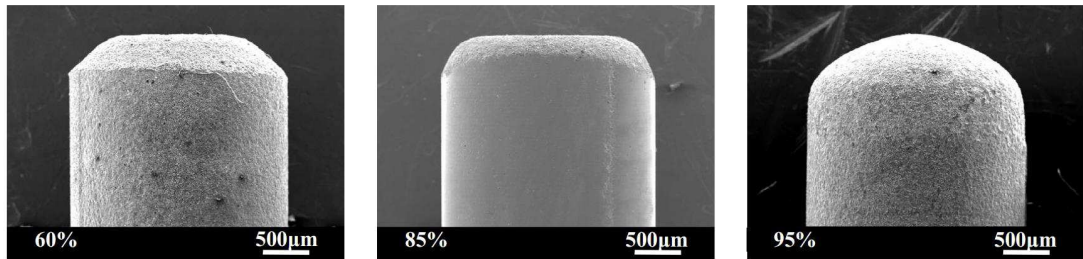


Figure 28: TWR varied with the relative density of the tool electrode (SEM images) [97].

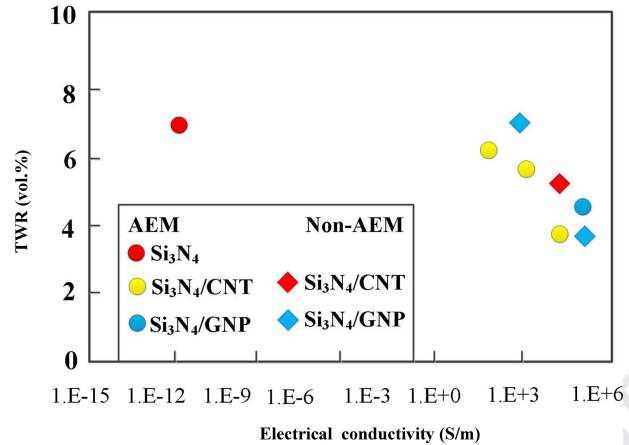


Figure 29: TWR was as a function of the electrical conductivity[17]

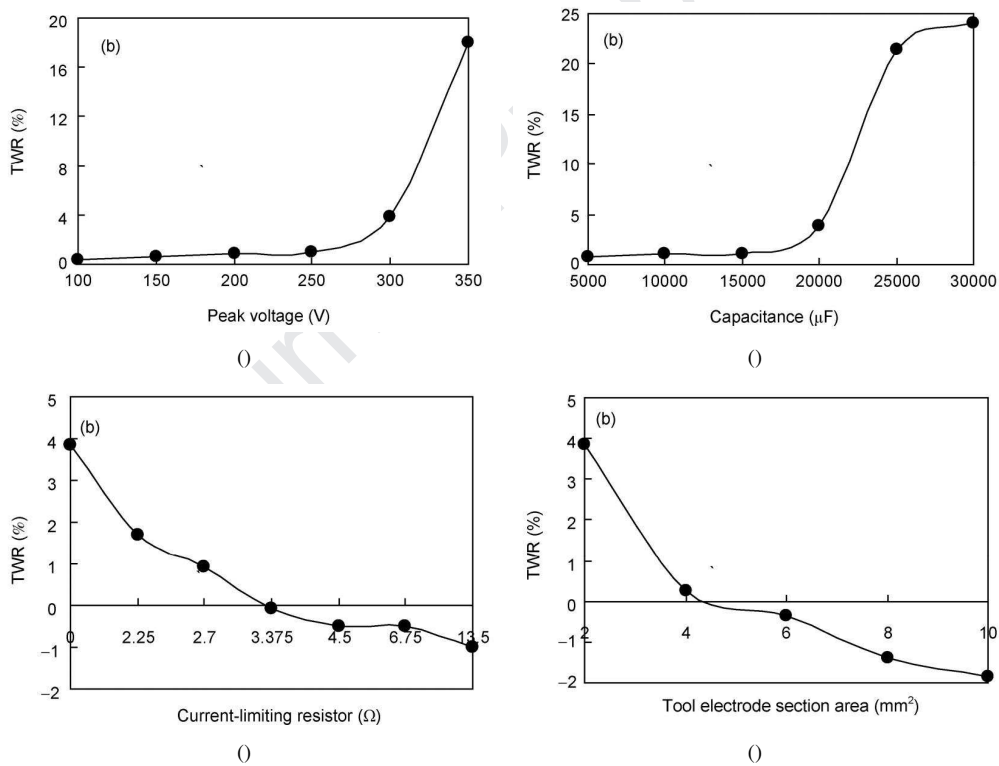


Figure 30: Effect of process parameters on the process performance of TWR; (a) effect of peak voltage on TWR; (b) effect of capacitance on TWR; (c) effect of current-limiting resistor on TWR; (d) effect of tool electrode section area on TWR [107].

4.3.2. Machining conductive ceramics

Sivasankar et al. studied the performance of various tool materials for EDM process of ZrB_2 advanced ceramics [108]. The performances of MRR and TWR for different tool materials were depicted in Fig.31. It can be revealed

that the tool wear rate (TWR) decreased (up to 40,000 W/m) with the product of thermal conductivity and melting point of tool material, and then increased. The reason for this increase was that tool materials had additional material loss due to the ablation behavior of ZrB₂. For the EDM of ZrB₂, these tools were selected according to the order of graphite, tantalum, tungsten, niobium, copper and molybdenum, but silver, brass and aluminum were not appropriate for EDM of it [107].

While machining of Si₃N₄/MWCNTs and Si₃N₄/TiN, Malek et al. found that both the machining performances (MRR and Ra) and TWR of Si₃N₄/MWCNTs were better than that of Si₃N₄/TiN while the process parameters kept unchanged (in Fig.32) [18]. The conclusion could be drawn from Fig.32 that TWR increased while the high MRR was desired. In addition, when the tool was used as the electrode of machining reference material, the TWR of machining Si₃N₄/TiN was about three times higher than that of machining Si₃N₄/MWCNTs.

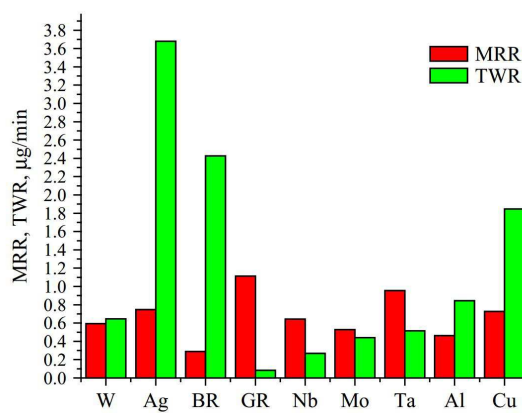


Figure 31: The performances of MRR and TWR for different tool materials [108].

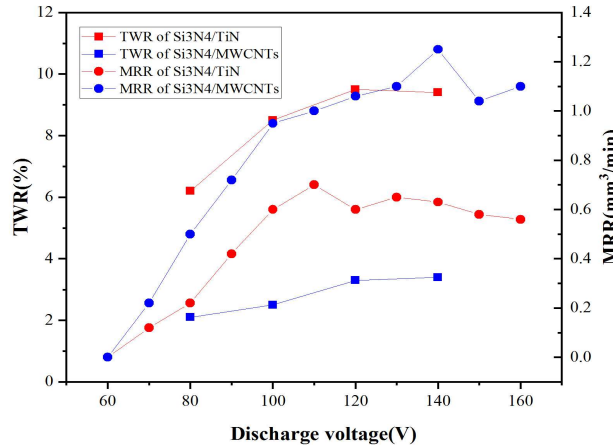


Figure 32: TWR and MRR were as a function of the discharge voltage, respectively [18].

Clijsters et al. also explored the effect of process parameters on TWR in the EDM process of Si-SiC [15]. They found that the significant parameter for TWR was the process parameters of discharge current and pulse-on time. Using the proposed machining strategy in roughing stage, the desired TWR (28%) could be acquired while discharge current, pulse-on time, gap voltage, and pulse period were 32A, 3.2μs, 200V, and 100μs, respectively. Moreover the relationship of TWR and MRR of each experiment was built, which was depicted in Figs 24 and 33. It could be also

drawn from Figs 24 and 33 that the desired TWR was achieved at high MRR.

Ji et al. investigated the influence of electrical resistivity on TWR of ZnO/Al₂O₃ in EDM [109]. The effect of the electrical resistivity on TWR in machining ZnO/Al₂O₃ was shown in Fig.34. The electrical resistivity of ZnO/Al₂O₃ ceramics varied from 6.3–324kΩ.cm with Al₂O₃ ranging from 0 to 2%, respectively. It can be found from Fig.34 that the TWR went up as the electrical resistivity declines. This was mainly attributed to the quick formation of pulse discharge channel as well as the increase of MRR [109]. Moreover, they studied the effect of the electrical resistivity and electrical process parameters on TWR, depicted in Fig.35, while machining ZnO/Al₂O₃ ceramics in the process of EDM [110]. Figure 35a presented that under the condition of high electrical transitivity, TWR increased with the increase of pulse-on time, while TWR decreased with the increase of pulse-on time under the condition of low electrical transitivity. This was because that a deposition layer, preventing the wear of tool electrode, could be formed on the surface of it during the high pulse-on time [110]. Under the same cutting condition, depicted in Fig.35b, TWR with pulse-off time of 200μs was lower than that with pulse-off time of 20μs, especially when the electrical resistivity was lower.

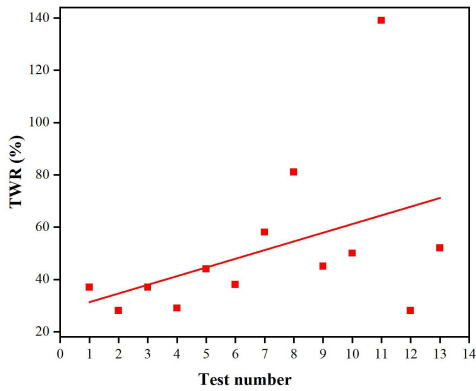


Figure 33: The relationship of TWR and MRR of each experiment while machining Si-SiC[15].

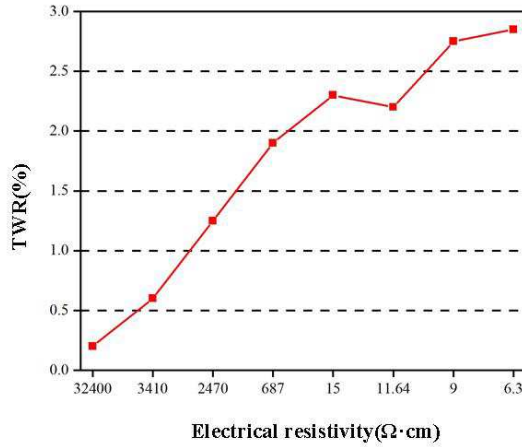


Figure 34: Effect of the electrical resistivity on TWR in machining ZnO/Al₂O₃ ceramics (Tool: +; pulse-on time: 20μs) [109].

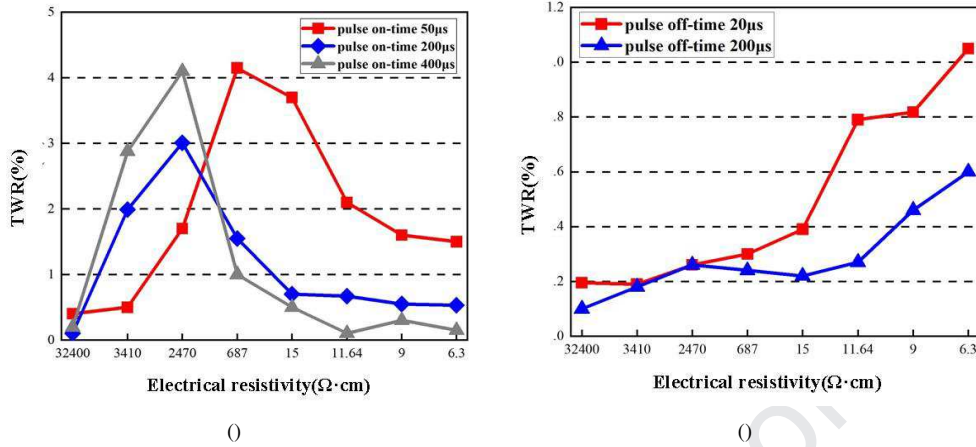


Figure 35: Effect of the electrical resistivity and electrical process parameters on TWR in machining ZnO/Al₂O₃ ceramics; (a) effect of the electrical resistivity and pulse-on time on TWR (discharge current: 50A; pulse-off time: 50 μs); (b) effect of the electrical resistivity and pulse-off time on TWR (discharge current: 50A; pulse-on time: 200 μs) [110].

4.3.3. Summary

EDM is a kind of precision machining, and TWR directly affects the machining accuracy of workpiece (advanced ceramics). Therefore, the TWR, MRR, and surface roughness (Ra) need to be comprehensively considered in this machining process. It could be concluded that the TWR, in most instances, was conflicted with that of MRR or surface roughness Ra [15, 18, 107, 110]. Hence, it was a feasible way to achieve multi-objective optimization by optimizing process parameters. However, this method could only improve the performance of TWR in a limited range, and it achieved the desired value at the expense of other performance, such as the MRR and Ra. In machining Si₃N₄ (non-conductive ceramics), the TWR was as a function of the electrical conductivity, and it decreased with the increase of conductivity of materials [17]. In addition, the TWR varied with the relative density of the tool electrode in machining ZrO₂ (non-conductive ceramics) [97]. For machining ZrB₂ (conductive ceramics), the materials of tool electrode were critical to the TWR, and graphite material was the best among the nine materials [108]. When cutting ZnO/Al₂O₃ (conductive ceramics), the experiment results showed that the TWR increased with the decrease of electrical resistivity [109]. These results confirmed that the materials (both non-conductive ceramics and conductive ceramics) and its properties of tool electrode had a significant effect on the performance of TWR. As for TWR optimization problem, these methods were based on machining mechanism in the EDM process of advanced ceramics. Therefore, it was more promising than multi-objective optimization method.

4.4. Surface topography and micro-structures

4.4.1. Machining non-conductive ceramics

The conductivity of ceramics is always most important factor for machining characteristics of EDM process. The surface recast layer generated in the EDM process of non-conductive ceramics were completed investigated by Banu et al.[111], and they analyzed recast layer hardness of zirconium oxide (ZrO₂) during the micro-EDM process of micro-channels based on assisting electrode method. Different conductive material adhesive coatings, namely Au, Cu and Au-Cu combination, were used as assisting electrodes to test their machinability in the micro-EDM process of ZrO₂. As shown in Fig.36, the SEM results revealed that the surface integrity of zirconia could be developed by using Cu adhesive as assisting electrode and positive polarity machining in the EDM process.

4.4.2. Machining conductive ceramics

When the conductive phase being added, the conductivity of ceramic composites can be developed to meet the requirement of EDM process. Due to the thermal shock and residual stress on the machined surface generated during the EDM process [112, 113, 114], Hu [115] and Patel [116] both conducted to study surface and subsurface damage like micro cracks and loose grains in EDM of Ti_3SiC_2 and $\text{Al}_2\text{O}_3\text{-SiC}_w\text{-TiC}$ ceramic composites. Hu found that the surface defects led to about 25% of strength degradation and scatter in the machined sample even though Ti_3SiC_2 having excellent damage tolerance due to the effect of nano-layered micro-structure, and Patel revealed that rough machining resulted in thermal erosion and bad surface integrity as well as small MRR at lower current range, resulting in few surface cracks or defects. The selected electrode materials of EDM could affect the surface micro structures and compositions. Zhang [117] observed the molybdenum of wire electrode was transferred to the machined surface via SEM, EDS, and XRD analysis because of a spark discharge reaction like melting and thermal spalling occurring between electrode and workpiece when conductive $\text{TiN/Si}_3\text{N}_4$ nanocomposite ceramics were processed by wire EDM. On the contrary, when the copper electrode was used to process TiB_2 ceramics, only few copper but some carbon and oxygen particles attached on the machined surface of TiB_2 specimens, which was attributed to retention of the dielectric fluid during the cooling process [118].

Tak et al. [119] evaluated the machining characteristics of micro-EDMed $\text{Al}_2\text{O}_3/\text{CNTs}$ ceramic composites, and they conducted a series of experiments to reveal that the conductivity of the ceramics and homogeneous distribution of CNTs in the matrix directly affects the machining accuracy and surface quality. Moreover, Singh et al. [120, 121] focused on studying surface characteristics including debris size, porous behavior, crack formation and propagation on the recast layer generated by the micro/wire-EDM process of MWCNT- Al_2O_3 composites. As for micro-EDM process, they found that the rotation speed of the tool electrode is a critical factor affecting surface quality: an increasing rotation speed boosted the longer and deeper cracks whereas decreased the recast layer formation as well as to some extent relieved porous behavior. As for WEDM process, in order to achieve better surface characteristics, they proposed multi-pass cutting strategy to smoothen the machined surface through removing the adhesive debris and cracks. A fine recast layer with sparse porous structure and few cracks could be obtained as shown in Fig.37. Also for improving the surface integrity of the electrical discharge machining ceramic composites, Deng et al. [122] implemented ultrasonic and abrasive blasting surface finishing to remove the distinct damage layer on the specimen of $\text{Al}_2\text{O}_3/\text{TiC}$ and $\text{Si}_3\text{N}_4/\text{TiC}$, which could result in a better strength and Weibull modulus.

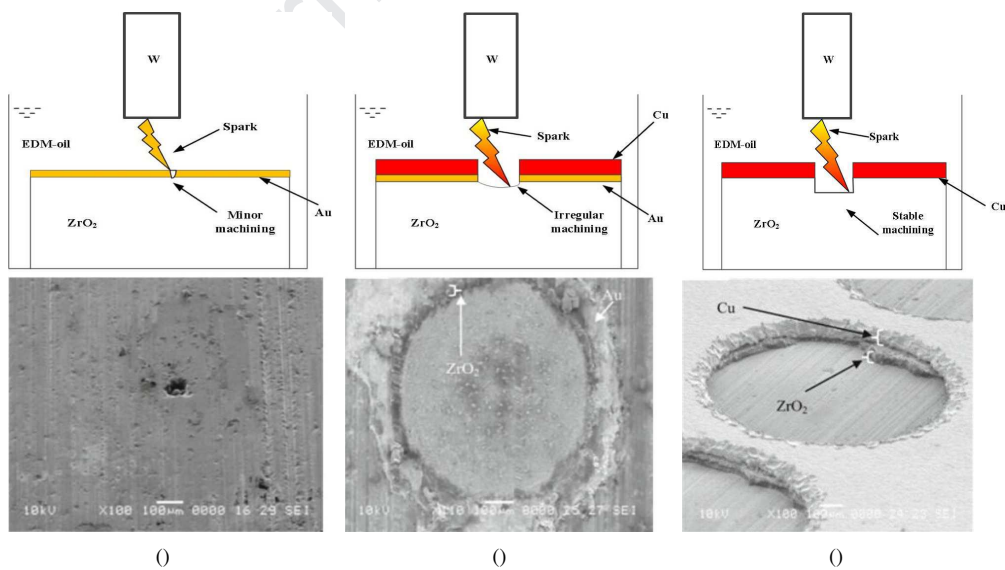


Figure 36: Machining schematic diagram and SEM images of machined ZrO_2 samples: b Au coating, c adhesive Cu foil and Au coating, and d adhesive Cu foil [111].

4.4.3. Summary

Surface integrity and microstructure are one of important machining performance indicators, which directly affect mechanical properties of machined surface by EDM process. As for EDM-AE process of non-conductive ceramics, assisting electrode materials would attach on the recast layer of machined surface and affect properties of substrate materials [111]. Thus the selection of appropriate materials of AE, thickness of AE, formation mechanism of AE, and its application method play significant role in the surface integrity of EDM process. As for EDM process of conductive ceramic composites, many researchers investigated surface characteristics including surface monograph, debris size, porous behavior, crack formation and propagation on the recast layer, and lots of methods, like multi-pass cutting [120], rotating the tool electrode [121], regulating the amount of conductive phase materials [119], ultrasonic and abrasive assisted [122], were proposed to improve the surface integrity.

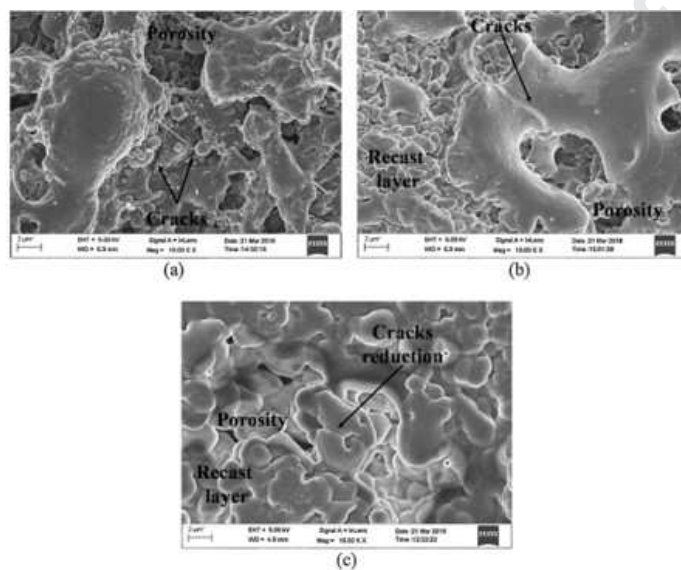


Figure 37: Comparison of porous structure and cracks propagation reduction with number of passes in (a) single pass, (b) three pass & (c) five pass [121].

5. New hybrid machining techniques

In order to achieve the excellent machining performance with high MRR, low EWR, and fine surface integrity during the EDM process of advanced ceramics, hybrid machining technology, which combines two or more machining processes conducted simultaneously or in a serial manner [123], has recently attracted significant interests and attentions from lots of researchers. Hybrid EDM processes equip with comprehensive advantages of different process techniques, so they provide more opportunities and applications for efficiently machining advanced ceramics.

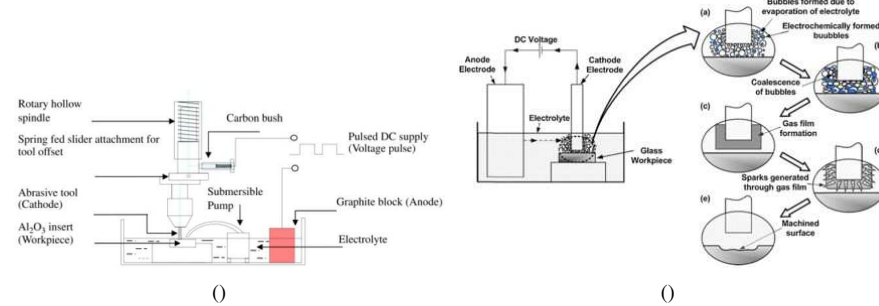


Figure 38: Schematic diagram of ECDM setup and material removal mechanisms: (a) Setup for drilling in ECDM [124]; (b) Material removal mechanisms in ECDM via forming gas film and associated spark machining [125].

ECDM: For sake of machining non-conductive ceramics [126], electrochemical discharge machining (ECDM) was proposed to combine electrochemical machining (ECM) and EDM on a single platform as shown in Fig.38 [124, 125]. The material removal mechanism of ECDM was that spark discharges between the cathode electrode and the non-conductive workpiece occurred through gas film generated from evaporation of electrolyte (be always NaOH and KOH due to less hazardous), while the electrochemical process dissolved the workpiece in the electrolyte solution [125]. This hybrid machining process could improve the MRR and machining accuracy of typical non-conductive hard brittle materials like glass and ceramics due to merge advantages of ECM and EDM.

Mechanical machining and EDM: The combination of mechanical machining (like milling, turning, and grinding) and EDM was implemented to process conductive hard and brittle materials, such as metal matrix composites and conductive ceramics. Ji et al. [127, 128] combined end electric discharge (ED) milling and mechanical grinding to effectively process a large surface area of SiC ceramic. As shown in Fig.39, this hybrid process equipped a turntable with several circumferential uniformly-distributed cylindrical copper electrodes and abrasive sticks as the tool, so end ED milling and mechanical grinding could alternately work on the workpiece to achieve rough (EDM) and finish (mechanical grinding) machining successively so as to improve MRR and surface quality under fine working environmental practice. Baghel et al. [129] proposed a similar hybrid process integrating diamond grinding and electro-discharge machining of TiN-Al₂O₃ ceramic composite to achieve higher MRR and better surface integrity. As shown in Fig.40, sparks discharges of EDM remove materials by melting and vaporization while high speed grinding efficiently removed both thermal softened and recast layer on the machined surface to achieve a better surface integrity.

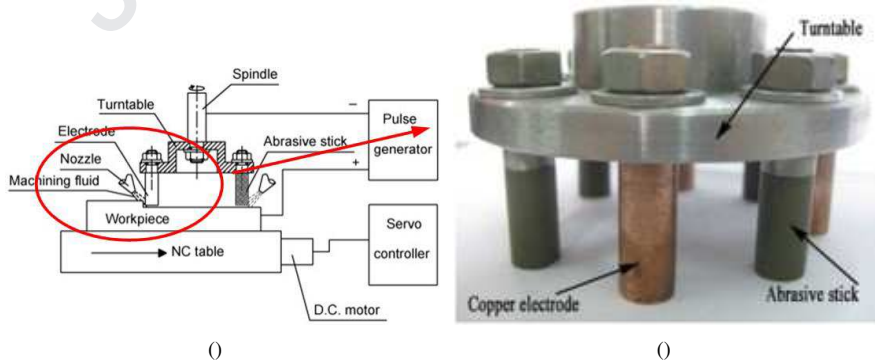


Figure 39: Schematic diagram of end ED milling and mechanical grinding [127, 128].

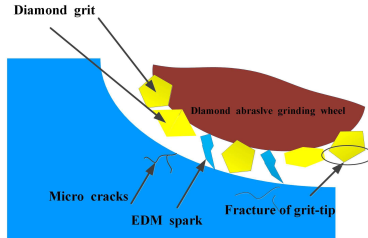


Figure 40: Mechanism of diamond grinding assisted electro-discharge machining [129].

Ultrasonic-assisted EDM: Ultrasonic waves can be not only used to smoothen material surface in the finish machining, but also widely applied as assisting method to enhance machining performances of many machining techniques (such as turning, milling, laser cutting, molding, EDM, WEDM) [130]. Ultrasonic vibration was employed in the EDM process to promote debris removal from the discharge gap, which helped clean the discharge area, stabilize the discharge status, and increase machining efficiency [131, 132]. Praneetpongung et al. [133] and Schubert et al. [134] proposed a hybrid process combining ultrasonic vibration and EDM (USEDm) with the assisting electrode to machine non-conductive ceramics (like Si_3N_4 and ZrO_2) with high stability and efficiency. Besides, Praneetpongung et al. [133] adopted direct ultrasonic vibration assisted method equipping with abrasives (seen in Fig.41) to polish conductive layers and craters and achieve good surface roughness. Schubert et al. [134] developed direct ultrasonic vibration (USV) assisted to the workpiece and indirect USV assisted to the dielectric aligned to the machining zone (seen in Fig.42) in the micro ED machining of non-conductive ZrO_2 ceramics. Liew et al. [135] also implemented USV assisted micro-EDM in the dielectric fluid to fabricate deep micro-holes SiC ceramics. As shown in Fig.43, this hybrid process could induce oscillation of cloud cavitation bubbles to take the debris away from machined surface under the effect of stirring and cavitation. The development of indirect ultrasonic vibration processing of non-conductive ceramic materials with high aspect ratio has brought great potential for the fabrication of advanced ceramic micro components with complex and high precision.

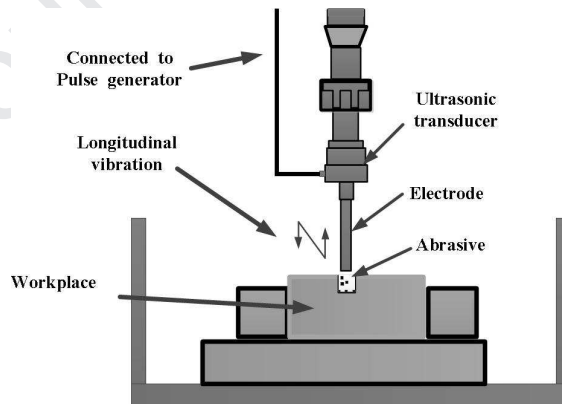
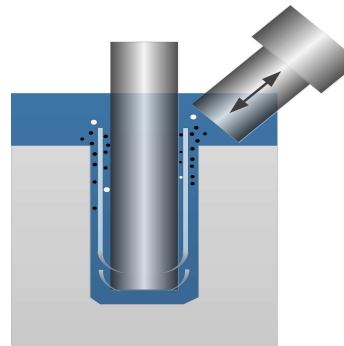
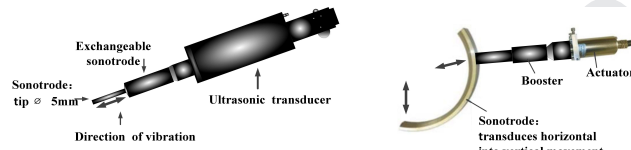


Figure 41: Schematic diagram of ultrasonic vibration assisted EDM with abrasives [133].



(a) Schematic diagram of indirect USV assisted micro-EDM



(b) Equipment and setup of indirect USV assisted micro-EDM

Figure 42: Schematic diagram and equipment of indirect USV assisted micro-EDM [134].

Magnetic field-assisted EDM: In the hybrid process of magnetic field (MF) assisted EDM, the external magnetic field could not only confine the radius of plasma channel based on the Larmor Radius Principle as well as increase the energy intensity of the plasma by creating smaller discharge spots and more electron collisions, but also improve the stability of plasma channel in electrical discharge process [131, 136]. Rattan et al. [137] developed MF assisted traveling wire electrochemical spark machining (MF-TWECSM) process combining wire-EDM and ECM process to machine electrically insulated materials. The magnetic field aligned to machining zone (seen in Fig.44) could apparently improve circulation of electrolyte and obtain high MRR and better machined surface with less overcut and heat affected zone.

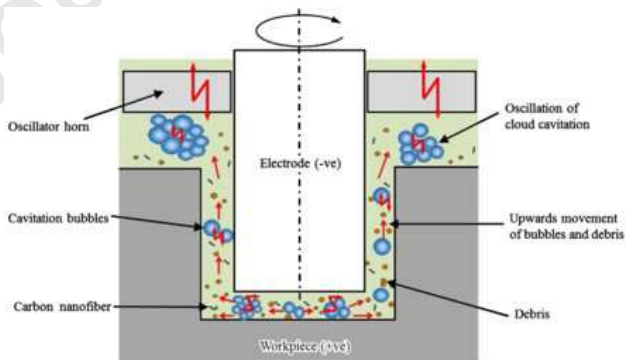


Figure 43: Schematic model for debris removal through the cavitation assisted micro-EDM of a deep micro-hole [135].

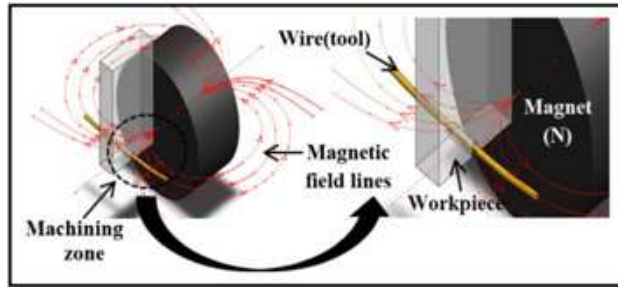


Figure 44: Schematic arrangement of the permanent magnet, wire electrode, and workpiece in MF-TWECSM process [137].

6. Outlook of future work

As the application of advanced ceramics continues to expand, the researches on its processing technology are also increasing, especially the EDM technology. Although the current researches on EDM process of advanced ceramic materials spread out, on the whole, the machining process still needs to be improved. In order to make EDM come to be an effective manufacturing process of conductive and non-conductive advanced ceramics, lots of related works could be carried out in the future. The following conclusions are drawn to present some future developments and challenges in the EDM process of advanced ceramics.

- For the EDM of advanced non-conductive ceramic materials, the selection of appropriate materials of auxiliary electrode (AE), thickness of AE, formation mechanism of AE, and its application method may contribute to the development of its processing technology. However, it turns to be complicated and difficult to select appropriate auxiliary electrode for different ED machining ceramics which is suitable for the specific industrial application, because it is necessary to comprehensively consider many factors including material properties of ceramics and AE, size and formation mechanism of AE, and machining performance indicators, which need lots of numerical and experimental researches and establish a process database for different non-conductive ceramics. In addition, the conductivity of the advanced ceramic materials can be regulated by adding a conductive phase material, but the inherent characteristics of ceramics have to be influenced by forms and amounts of added conductive phases, and the new characteristics of ceramic composites with conductive phase should be tested and verified by lots of experiments. Therefore, how to optimize the volume fraction of the second phase material should be investigated in specific application areas.
- Pulse on time was one of the most important parameters that affect the performance of machining advanced non-conductive ceramics in EDM. Therefore, it is also necessary to develop an enhanced pulse generator specially designed for this EDM process. By precisely controlling the pulse-on time, the characteristic parameters of the conductive film attached on the non-conductive will be affected, which is the key point of EDM for such ceramic materials [138]. Therefore, it is necessary to establish a mathematic model to quantitatively describe the growth of the conductive film for different types of ceramics with EDM process parameters. Also, the relationship between the pulse generator and the formation of the conductive film will be further investigated.
- At present, most of the existing studies on EDM of advanced ceramics focus on the feasibility and performance of experimental researches. The main challenge is to better describe the physical process of ED machining these materials using accurate numerical models. In addition, the physical models should be proposed to study the growth of conductive film and the subsequent material removal process, to visualize the formation of surface micro cracks, and to figure out thermal process of vaporization and spalling. These models may be established via precisely describing thermal fracture process of advanced ceramics to molecular dynamics and finite element method.

- The evaluation of machining performances is also important to determine whether the manufacturing process is suitable for a particular application. Since the EDM of non-conductive ceramics is finished by depositing secondary conductive carbon film on the surface, it is necessary to test the mechanical and physical characteristics of machined surface to evaluate the performance of machined components. The hardness, residual stress, micro-structures, and conductivity of the machined surface after EDM of advanced ceramic materials should be further studied [139, 140, 141]. In addition, due to the low efficiency and high electrode wear of EDM, it is necessary to consider the overall effect of process parameters on various performance indicators including MRR, EWR, and machining quality.
- Intelligent EDM process of advanced ceramics shall be the future developing trend, which is very important to determine the best combination of processing parameters in the EDM of advanced ceramics, especially in new ceramics materials [142, 143, 144]. The mathematic model or artificial neural network (ANN) model can be established based on the data of experiments. Considering single or multi-objective optimization of EDM process, the optimal parameters combinations for different types of ceramics are rapidly and accurately obtained by using genetic algorithm (GA), particle swarm optimization (PSO), simulated annealing algorithm (SAA), wolf colony algorithm (WCA) and other hybrid intelligent optimization algorithms. The optimal parameters include not only the electrical parameters (discharge current, pulse-on time, pulse-off time, and etc.) of EDM, but also the non-electrical parameters, such as workpiece material (the density of materials, the secondary electro-conductive phases, and etc.), electrode material and machining fluid.
- Hybrid EDM processes comprehensive advantages of different process techniques, and they provide more opportunities and potentials for efficiently machining advanced ceramics. Thus researchers will continue to develop a new hybrid EDM technique for machining non-conductive advanced ceramics in the future. A typical hybrid EDM machining technique is a magnetic field assisted EDM (MF-EDM), which can confine the plasma channel and affect the formation of conductive film [136]. In addition, powder mixed electric discharge machining (PMEDM) has developed to finishing stage. Recently, the deposition with EDM(DEDM) technique has also been successfully implemented for metal materials, and this method possibly contributes to machining non-conductive ceramics. This requires an evaluation of the feasibility of DEDM of advanced ceramics to enhance their applications and related scopes.
- The EDM process of ceramics is still considered as hazardous to the operators as well as to the environment due to considerable amount of harmful emissions including poisonous aerosols, gases, debris, and noise during high-energy pulse discharge reaction between anode and cathode [136, 145, 146]. The generation of hazardous substances from the EDM process is mainly dependent on material removal mechanism, dielectric fluid, tool material and workpiece material. Thus, considering the effect of different process parameters and types of advanced ceramics, sustainability of EDM process of ceramics should be investigated and optimized to relieve negative environmental impact.
- Finally, most of the researches focused on the feasibility and machinability of various advanced ceramics. Few researches focus on the ceramic parts or components, which are applied in industry by EDM/micro-EDM. At present, researchers will face the challenge of expanding the application filed by machining industrial parts or components in some cost-effective techniques. Therefore, the future research should focus on the high ratio (height/diameter) micro-holes, complex 3D micro-features and precise functional parts on advanced ceramics.

Acknowledgements

This research is supported by National Natural Science Foundation of China (51705171). In addition, this research is also supported by Local Innovative and Research Teams Project of Guangdong Pearl River Talents Program (2017BT01G167) and Natural Science Foundation of Henan Province (182300410170).

- [1] J. Wang, R. Stevens, Zirconia-toughened alumina (ZTA) ceramics, journal of materials science, J. Mater. Sci. 24 (10) (1989) 3421–3440.
- [2] M. Szutkowska, M. Boniecki, Subcritical crack growth in zirconia-toughened alumina (ZTA) ceramics, J. Mater. Process. Technol 175 (1-3) (2006) 416–420.
- [3] A. H. D. Aza, J. Chevalier, G. Fantozzi, M. Schehl, R. Torrecillas, Slow-crack-growth behavior of zirconia-toughened alumina ceramics processed by different methods, J. Am. Ceram. Soc. 86 (1) (2003) 115–120.

- [4] M. A. Elezz, F. Kern, R. Gadow, Manufacturing of ZTA composites for biomedical applications, ICET2012.
- [5] M. Ahlhelm, P. Gnther, U. Scheithauer, E. Schwarzer, A. Michaelis, Innovative and novel manufacturing methods of ceramics and metal-ceramic composites for biomedical applications, *J. Eur. Ceram. Soc.* 36 (12) (2016) 2883–2888.
- [6] A. L. D. Skury, S. Chagas, S. N. Monteiro, Use of silicon nitride as an additive in the production of cbn compacts for cutting tools, *Mater. Sci. Forum* (2012) 727–728, 1040–1044.
- [7] L. Y. Cao, Z. H. Wang, Z. Yin, K. Liu, J. T. Yuan, Investigation on mechanical properties and microstructure of silicon nitride ceramics fabricated by spark plasma sintering, *Mater. Sci. Eng., A* 731 (2018) 595–602.
- [8] A. Laouissi, M. A. Yallese, A. Belbah, S. Belhadi, A. Haddad, Investigation, modeling, and optimization of cutting parameters in turning of gray cast iron using coated and uncoated silicon nitride ceramic tools. based on ann, rsm, and ga optimization, *Int. J. Adv. Manuf. Tech.* 101 (2019) 523–548.
- [9] <http://www.line-machine.com/product/introduce.php?dirid=77&pid=2600000>.
- [10] H. Li, S. Zhang, X. M. Wang, J. H. Lin, B. L. Kou, Medium-term results of ceramic-on-polyethylene Zweymller-Plus total hip arthroplasty, *Hong Kong Academy of Medicine* 23 (4) (2017) 333–339.
- [11] R. Civinini, P. D. Biase, C. Carulli, F. Matassi, M. Innocenti, The use of an injectable calcium sulphate/calcium phosphate bioceramic in the treatment osteonecrosis of the femoral head, *Int. Orthop* 36 (8) (2012) 1583–1588.
- [12] A. D. Heiner, C. R. Mahoney, Fracture of a biolox delta ceramic femoral head articulating against a polyethylene liner: a case report, *JBJS Case Connector* 4 (4) (2014) e97–e97.
- [13] G. Magnani, A. Brillante, Effect of the composition and sintering process on mechanical properties and residual stresses in zirconia alumina composites, *J. Eur. Ceram. Soc.* 25 (2005) 3383–3392.
- [14] K. Liu, D. Reynaerts, B. Lauwers, Influence of the pulse shape on the edm performance of Si₃N₄-TiN ceramic composite, *CIRP Ann-Manuf Techn* 58 (1) (2009) 217–220.
- [15] S. Clijsters, K. Liu, D. Reynaerts, B. Lauwers, Edm technology and strategy development for the manufacturing of complex parts in SiSic, *J. Mater. Process. Technol* 210 (4) (2010) 631–641.
- [16] H. C. Li, Z. L. Wang, Y. K. Wang, H. Z. Liu, Z. X. Zhao, Micro-EDM and micro-USM combined milling of ZrB₂-SiC-graphite composite for 3d micro-cavities, *Int. J. Adv. Manuf. Technol* 99 (9-12) (2018) 2535–2645.
- [17] D. Hanaoka, Y. Fukuzawa, C. Ramirez, P. Miranzo, M. I. Osendi, M. Belmonte, Electrical discharge machining of ceramic/carbon nanos-tructure composites, *Procedia CIRP* 6 (2013) 95–100.
- [18] O. Malek, J. Gonzalez-Julian, J. Vleugels, W. Vanderauwera, B. Lauwers, M. Belmonte, Carbon nanofillers for machining insulating ceramics, *Mater Today* 14 (2011) 496–501.
- [19] Y. Fukuzawa, N. Mohri, H. Gotoh, T. Tani, Three-dimensional machining of insulating ceramics materials with electrical discharge machining, *Trans Nonferrous Met Soc China* 19 (2009) s150–s156.
- [20] <https://www.ceramtec.com/biolox/materials/material-combinations/>.
- [21] T. Tani, Y. Fukuzawa, N. Mohri, N. Saito, M. Okada, Machining phenomena in WEDM of insulating ceramics, *J. Mater. Process Technol* 149 (2004) 124–128.
- [22] M. Schwartz, Handbook of structural ceramics, *Int. J. Prod. Res.* 42 (4) (1992) ISBN: 0070557195.
- [23] I. P. Tuersley, A. Jawaid, I. R. Pashby, Review: various methods of machining advanced ceramic materials, *J. Mater. Process Technol* 42 (4) (1994) 377–390.
- [24] Cramton, C. Roger, New structural materials technologies: opportunities for the use of advanced ceramics and composites, 1986.
- [25] S. Bortz, Reliability of ceramics for heat engine applications. ceramics for high-performance, Applications III, Springer US. (1983) 445–473.
- [26] G. Magnani, G. L. Minoccari, L. Pilotti, Flexural strength and toughness of liquid phase sintered silicon carbide, *Ceram. Int.* 26 (5) (2000) 495–500.
- [27] P. Pawar, B. R., A. Kumar, An overview of machining process of alumina and alumina ceramic composites, *J. Am. Oil Chem. Soc.* 3 (1) (2015) 10–15.
- [28] M. L. Herrera, R. W. Hartel, Effect of processing conditions on physical properties of a milk fat model system: Rheology, *J. Am. Oil. Chem. Soc.* 77 (11) (2000) 1197–1205.
- [29] A. Sabur, M. Y. Ali, M. A. Maleque, A. A. Khan, Investigation of material removal characteristics in edm of nonconductive ZrO₂ ceramic, *Procedia Eng.* 56 (2013) 696–701.
- [30] C. Srikanth, G. M. M. Madhu, Synthesis, characterization and properties evaluation of ZrO₂ and its composites a review, *SSRN Electronic Journal*.
- [31] B. Basu, G. Raju, A. Suri, Processing and properties of monolithic TiB₂ based materials, *Metall. Rev.* 51 (6) (2013) 352–374.
- [32] A. Tampieri, A. Bellosi, Oxidation resistance of aluminactitanium nitride and aluminactitanium carbide composites, *J. Am. Ceram. Soc.* 75 (6) (1992) 1688–1690.
- [33] A. N. Samant, N. B. Dahotre, Laser machining of structural ceramics a review, *J. Eur. Ceram. Soc.* 29 (6) (2009) 969–993.
- [34] I. Tuersley, A. Jawaid, I. Pashby, Various methods of machining advanced ceramic materials, *J. Mater. Process. Technol* 42 (1994) 377–390.
- [35] A. Fernandez-Valdivielso, L. Lpez de Lacalle, G. Urbikain, A. Rodriguez, Detecting the key geometrical features and grades of carbide inserts for the turning of nickel-based alloys concerning surface integrity, *Proc. Inst. Mech. Eng. Part C J. Mech. Eng. Sci.* 230 (2016) 3725–3742.
- [36] B. Zhang, X. L. Zheng, H. Tokura, M. Yoshikawa, Grinding induced damage in ceramics, *J. Mater. Process. Technol.* 132 (1) (2003) 353–364.
- [37] H. P. Kirchner, Damage penetration at elongated machining grooves in hotpressed Si₃N₄, *J. Am. Ceram. Soc.* 67 (2) (2010) 127–132.
- [38] J. P. Choi, B. H. Jeon, B. H. Kim, Chemical-assisted ultrasonic machining of glass, *J. Mater. Process. Technol.* 191 (1-3) (2007) 153–156.
- [39] P. Gudimetla, J. Wang, W. Wong, Kerf formation analysis in the abrasive waterjet cutting of industrial ceramics, *J. Mater. Process. Tech.* 128 (1-3) (2002) 123–129.
- [40] J. M. Park, S. C. Jeong, H. W. Lee, H. D. Jeong, E. S. Lee, A study on the chemical mechanical micro-machining (C3M) process and its application, *J. Mater. Process. Technol.* 130-131 (2002) 390–395.

- [41] Y. X. Yao, B. Wang, J. H. Wang, H. L. Jin, Y. F. Zhang, S. Dong, Chemical machining of zerodur material with atmospheric pressure plasma jet, CIRP Ann-Manuf Techn 59 (1) (2010) 337–340.
- [42] M. A. Montes-Moran, F. W. J. V. Hattum, J. P. Nunes, A. Martinez-Alonso, J. M. D. Tascon, C. A. Bernardo, A study of the effect of plasma treatment on the interfacial properties of carbon fibre-thermoplastic composites, Carbon 43 (8) (2005) 1795–1799.
- [43] A. S. Kuar, B. Doloi, B. Bhattacharyya, Modelling and analysis of pulsed Nd:YAG laser machining characteristics during micro-drilling of zirconia (ZrO_2), Int. J. Mach. Tool. Manu. 46 (12-13) (2006) 1301–1310.
- [44] B. Shi, Y. Dai, X. Xie, S. Li, L. Zhou, Arc-enhanced plasma machining technology for high efficiency machining of silicon carbide, Plasma. Chem. Plasma. P. 36 (3) (2016) 891–900.
- [45] B. Shi, Y. Dai, X. Xie, S. Li, L. Zhou, An experimental study on arcing in arc-enhanced plasma machining technology for etching of silicon carbide ceramics, Int. J. Adv. Manuf. Tech. 89 (2017) 3517–3525.
- [46] P. S. Spinney, D. G. Howitt, R. L. Smith, S. D. Collins, Nanopore formation by low-energy focused electron beam machining, Nanotechnol-ogy 21 (37) (2010) 375–401.
- [47] H. M. Kim, S. Y. Cho, K. B. Kim, Nanopore formation in tin membranes by the focused electron beam of a transmission electron microscope, J. Vac. Sci. Technol. B. 33 (6) (2015) 06F502.
- [48] Z. X. Jia, J. H. Zhang, X. Ai, High quality machining of engineering ceramics, Key Eng. Mater. (1995) 108–110, 155–164.
- [49] S. Lei, Y. C. Shin, F. P. Incropera, Deformation mechanisms and constitutive modeling for silicon nitride undergoing laser-assisted machining, Int. J. Mach. Tool. Manu. 40 (15) (2000) 2213–2233.
- [50] Y. Tian, Y. C. Shin, Thermal modeing for laser-assisted machining of silicon nitride ceramics with complex features, J. Manuf. Sci. E-T 128 (2) (2006) 425–434.
- [51] P. C. Pandey, H. S. Shan, Modern Machining Processes McGraw Hill, 1980.
- [52] S. W. Lee, Y. S. Oh, A study on dry electrical discharge machining process, International Conference on Smart Manufacturing Application. IEEE. (2008) 234–238.
- [53] S. Boopathi, K. Sivakumar, Experimental investigation and parameter optimization of near-dry wire-cut electrical discharge machining using multi-objective evolutionary algorihtm., Int. J. Adv. Manuf. Tech. 67 (9-12) (2013) 2639–2655.
- [54] Jagadish, A. Ray, Optimization of process parameters of green electrical discharge machining using principal component analysis (pca), Int. J. Adv. Manuf. Tech. 87 (5-8) (2016) 1299–1311.
- [55] C. Martin, B. Cales, P. Vivier, Electrical discharge machinable ceramic composites, Mater. Sci. Eng. A 109 (89) (1989) 351–356.
- [56] C. Wei, L. Zhao, D. Hu, J. Ni, Electrical discharge machining of ceramic matrix composites with ceramic fiber reinforcements, Int. J. Adv. Manuf. Tech. 64 (1-4) (2013) 187–194.
- [57] S. Salehi, O. V. D. Biest, J. Vleugels, Electrically conductive ZrO_2 -TiN composites, J. Eur. Ceram. Soc. 26 (15) (2006) 3173–3179.
- [58] N. Mohri, Y. Fukuzawa, T. Tani, Assisting electrode method for machining insulating ceramics, CIRP Ann-Manuf Techn 45 (1) (1996) 201–204.
- [59] T. Tani, Y. Fukuzawa, N. Mohri, Machining phenomena in WEDM of insulating ceramics, J. Mater. Process Technol 149 (1-3) (2004) 124–128.
- [60] Y. Fukuzawa, A. Imata, Y. Kaneko, T. Harada, Mechanical strength of the wire edmed insulating ZrO_2 ceramics by assisting electrode method, Proceedings of the 15th International Symposium on Electromachining 165–169.
- [61] A. Muttamara, Y. Fukuzawa, N. Mohri, T. Tani, Effect of electrode material on electrical discharge machining of alumina, J. Mater. Process Technol 209 (5) (2009) 2544–2552.
- [62] C. Praneetpong, Y. Fukuzawa, S. Nagasawa, K. Yamashita, Effects of the EDM combined ultrasonic vibration on the machining properties of Si_3N_4 , Mater. Trans. 51 (11) (2010) 2113–2120.
- [63] G. Kucukturk, C. Cogun, A new method for machining of electrically nonconductive workpieces using electric discharge machining technique, Mach. Sci. Technol. 14 (2) (2010) 189–207.
- [64] C. L. Guo, J. Y. Pei, A. Pan, EDM of non-conductive ceramics with conductive magnetic powder (2005) ZL200510111502.2 [In Chinese].
- [65] N. F. Xu, A study of insulating ceramics SiO_2 machining by EDM, Med. Bull. Shanghai Jiaotong Univ. (2017) Master Dissertation [In Chinese].
- [66] T. Chisato, O. Keisaku, Electrochemical discharge machining (EDM) and micro hole machining, Proceedings of the National Congress of the electrical processing society (2005) 107–108.
- [67] Y. H. Liu, Z. X. Jia, J. C. Liu, Study on hole machining of non-conducting ceramics by gas-filled electrodischarge and electrochemical compound machining, J. Mater. Process Technol 69 (1-3) (1997) 198–202.
- [68] R. Snoeys, F. S. Dijck, Investigation of electro discharge machining operations by means of thermo-mathematical model, CIRP Ann 20 (1) (1971) 35–37.
- [69] F. S. Dijck, W. L. Dutre, Heat conduction model for the calculation of the volume of molten metal in electric discharges, J. Phys. D: Appl. Phys. 7 (6) (1974) 899.
- [70] J. V. Beck, Transient temperatures in a semi-infinite cylinder heated by a disk heat source, Int. J. Heat Mass Transfer 24 (10) (1981) 1631–1640.
- [71] J. V. Beck, Large time solutions for temperatures in a semi-infinite body with a disk heat source, Precis. Eng. 24 (1) (1981) 155–164.
- [72] D. D. DiBitonto, P. T. Eubank, M. R. Patel, Theoretical models of the electrical discharge machining process. I. A simple cathode erosion model, J. Appl. Phys. 66 (9) (1989) 4095–4103.
- [73] S. T. Jilani, P. C. Pandey, Analysis and modelling of edm parameters. precision engineering, Precis. Eng. 4 (4) (1982) 215–221.
- [74] S. T. Jilani, P. C. Pandey, An analysis of surface erosion in electrical discharge machining, Wear 84 (3) (1983) 275–284.
- [75] L. L. Yu, Research on mechanism and application of electrical discharge machining with synchronous servo double electrodes for non-conductive engineering ceramics, China University of Petroleum (East China).
- [76] Y. H. Liu, L. L. Yu, Y. L. Xu, R. J. Ji, Q. Y. Li, Numerical simulation of single pulse discharge machining insulating Al_2O_3 ceramic proc, Engineering Manufacture 223 (1) (2008) 55–62.
- [77] M. A. Singh, K. Das, Thermal simulation of machining of alumina with wire electrical discharge machining process using assisting electrode,

- J. Mech. Sci. Technol. 32 (1) (2018) 333–343.
- [78] R. A. Mahdavinejad, M. Tolouei-Rad, H. Sharifi-Bidgoli, **Heat transfer analysis of EDM process on silicon carbide**, Int. J. Numer. Method. H. 15 (5) (2005) 483–502.
- [79] F. Yasushi, N. Sigeru, K. Yo, S. Hiroshi, Y. Kazusige, **Effect of Interface Shape on Residual Stress Distribution in TiB₂-Ni Diffusion Bonding Material**, J. Japan. Inst. Metals 56 (7) (1992) 842–848.
- [80] K. K. Saxena, S. Agarwal, R. Das, **Evaluation of Micro-EDM (DM) Characteristics of Conductive Silicon Carbide Using a Coupled Thermo-Structural Process Model**, J. Adv. Mech. Des. Syst.
- [81] C. J. Ma, Experimental research and removal crater simulation of single pulse discharge for EDM of ZrB₂-SiC ceramic, J. Harbin Inst. Technol. (Engl. Ed.).
- [82] C. Pupaza, D. Ghiculescu, C. G. Opran, A model regarding material removal using fem at ultrasonic aided EDM of metal matrix composites, Mech Mater 760 (2015) 557–562.
- [83] S. Das, M. Klotz, **EDM simulation: finite element-based calculation of deformation, microstructure and residual stresses**, J. Mater. Process. Technol. 142 (2) (2003) 434–451.
- [84] J. Marafona, J. A. G. Chousal, **A finite element model of EDM based on the Joule effect**, Int. J. Mach. Tool. Manu. 46 (6) (2006) 595–602.
- [85] Y. Tahmasebipour, M. Ghereishi, **Finite-Volume Heat Transfer Model of the Nano Electrical Discharge Machining Process**, J. Nanoelectron. Optoelectron. 9 (2014) 601–607.
- [86] S. Banerjee, B. V. S. S. Prasad, **Numerical evaluation of transient thermal loads on a WEDM wire electrode under spatially random multiple discharge conditions with and without clustering of sparks**, Int. J. Adv. Manuf. Tech. 48 (5-8) (2010) 571–580.
- [87] B. Izquierdo, J. A. Snchez, S. Plaza, I. Pombo, N. Ortega, **A numerical model of the EDM process considering the effect of multiple discharges**, Int. J. Adv. Manuf. Tech. 49 (3-4) (2009) 220–229.
- [88] A. Tlili, N. B. Ghanem, F. Salah, **A contribution in EDM simulation field**, Int. J. Adv. Manuf. Tech. 79 (5-8) (2015) 921–935.
- [89] T. Lee, W. Lau, Some characteristics of electrical discharge machining of conductive ceramics, Mater. Manuf. Process 6 (1991) 635–648.
- [90] G. J. Zhang, J. W. Guo, W. Y. Ming, Study of the machining process of nano-electrical discharge machining based on combined atomistic-continuum modeling method, Appl. Surf. Sci. 290 (2014) 359–367.
- [91] B. Lauwers, J. P. Kruth, W. Liu, W. Eeraerts, B. Schacht, P. Bleys, Investigation of material removal mechanisms in edm of composite ceramic materials, J. Mater. Process. Technol. 149 (1-3) (2004) 347–352.
- [92] H. Huang, Z. Zhang, W. Ming, A novel numerical predicting method of electric discharge machining process based on specific discharge energy, Int. J. Adv. Manuf. Tech. 88 (1-4) (2017) 409–424.
- [93] L. Melk, M. L. Antti, M. Anglada, Material removal mechanisms by edm of zirconia reinforced mwcnt nanocomposites, Ceram. Int. 42 (5) (2016) 5792–5801.
- [94] Y. Pachaury, P. Tandon, **An overview of electric discharge machining of ceramics and ceramic based composites**, J. Manuf. Process. 25 (2017) 369–390.
- [95] Y. Fukuzawa, **Electrical discharge machining properties of noble crystals**, J. Mater. Process Technol 149 (1-3) (2004) 393–397.
- [96] Y. H. Liu, R. J. Ji, X. P. Li, L. L. Yu, H. F. Zhang, Q. Y. Li, **Effect of machining fluid on the process performance of electric discharge milling of insulating Al₂O₃ ceramic**, Int. J. Mach. Tool. Manu. 48 (9) (2008) 1030–1035.
- [97] Y. Fukuzawa, K. Yukihiko, K. Yamasita, **Machining properties of insulating ZrO₂ ceramics using porous copper electrodes**, Key Eng Mater 443 (2010) 608–613.
- [98] I. Puertas, C. J. Luis, **A study of optimization of machining parameters for electrical discharge machining of boron carbide**, Mater. Manuf. Processes 19 (6) (2004) 1041–1070.
- [99] I. Puertas, C. J. Luis, **Optimization of EDM conditions in the manufacturing process of B4C and wc-co conductive ceramics**, Int. J. Adv. Des. Manuf. Technol. 59 (5-8) (2012) 575–582.
- [100] D. F. Dauw, **On-line identification and optimization of Electro-Discharge Machining**, Production Engineering Machine Design & Automation.
- [101] K. M. Patel, P. M. Pandey, P. V. Rao, **Optimisation of process parameters for multi-performance characteristics in EDM of Al₂O₃ ceramic composite**, Int. J. Adv. Manuf. Tech. 47 (9-12) (2010) 1137–1147.
- [102] K. Bonny, P. D. Baets, J. Vleugels, A. Salehi, O. V. D. Biest, B. Lauwers, W. Liu, Influence of secondary electro-conductive phases on the electrical discharge machinability and frictional behavior of ZrO₂-based ceramic composites, J. Mater. Process Technol 208 (1-3) (2008) 423–430.
- [103] Y. S. Liao, Y. P. Yu, Study of specific discharge energy in wedm and its application, Int. J. Mach. Tool. Manu. 44 (12-13) 1373–1380.
- [104] W. Y. Ming, Z. Zhang, S. Y. Wang, H. Huang, D. L. Shen, Investigating the energy distribution of workpiece and optimizing process parameters during the edm of Al6061, Inconel718, and SDK72, Int. J. Adv. Manuf. Tech. 92 (1) (2017) 1–18.
- [105] K. K. Saxena, A. S. Srivastava, S. Agarwal, Experimental investigation into the micro-EDM characteristics of conductive SiC, Ceram. Int. 42 (1) (2016) 1597–1610.
- [106] K. M. Patel, P. M. Pandey, P. V. Rao, Determination of an optimum parametric combination using a surface roughness prediction model for EDM of Al₂O₃/SiCw/TiC ceramic composite, Mater. Manuf. Processes 24 (6) (2009) 675–682.
- [107] R. J. Ji, Y. H. Liu, Y. Z. Zhang, H. F. Zhang, X. P. Li, X. Dong, **An experimental research on single discharge machining of insulating ceramics efficiently with high energy capacitor**, Sci. China: Technol. Sci. 54 (6) (2011) 1537–1545.
- [108] S. Sivasankar, R. Jeyapaul, V. V. Banuprasad, **Performance study of various tool materials for electrical discharge machining of hot pressed ZrB₂** 8 (4) (2012) 505–523.
- [109] R. J. Ji, Y. H. Liu, R. Q. Diao, C. C. Xu, X. P. Li, B. P. Cai, Y. Z. Zhang, Influence of electrical resistivity and machining parameters on electrical discharge machining performance of engineering ceramics, Plos One 9 (11) (2014) e110775.
- [110] R. Ji, Y. Liu, R. Diao, Y. Zhang, F. Wang, B. Cai, C. Xu, Experimental research on electrical discharge machining characteristics of engineering ceramics with different electrical resistivities, Int. J. Adv. Manuf. Tech. 75 (9-12) (2014) 1743–1750.
- [111] A. Banu, M. A. Ali, M. Y. and Rahman, Micro-electro discharge machining of non-conductive zirconia ceramic: investigation of MRR and recast layer hardness, Int. J. Adv. Manuf. Tech. 75 (1-4) (2014) 257–267.
- [112] B. Ekmekci, Residual stresses and white layer in electric discharge machining(EDM), Appl. Surf. Sci. 253 (2007) 9234–9240.

- [113] Y. Zhang, Z. Zhang, G. Zhang, Reduction of energy consumption and thermal deformation in WEDM by magnetic field assisted technology, *Int. J. Pr. Eng. Man-GT* 7 (2) (2020) 391–404.
- [114] Y. Zhang, S. Guo, Z. Zhang, Simulation and experimental investigations of complex thermal deformation behavior of wire electrical discharge machining of the thin-walled component of inconel 718, *J. Mater. Process Technol* 270 (2019) 306–322.
- [115] C. Hu, Y. Zhou, Y. Bao, Material removal and surface damage in EDM of Ti3SiC2 ceramic, *Ceram. Int.* 34 (3) (2008) 537–541.
- [116] K. M. Patel, P. M. Pandey, P. V. Rao, Surface integrity and material removal mechanisms associated with the EDM of Al2O3 ceramic composite, *Int. J. Refract. Met. Hard Mater.* 27 (5) (2009) 200510111502.2 [In Chinese].
- [117] C. M. Zhang, Effect of wire electrical discharge machining (WEDM) parameters on surface integrity of nanocomposite ceramics, *Ceram. Int.* 40 (7) (2014) 9657–9662.
- [118] A. Torres, C. J. Luis, I. Puertas, Edm machinability and surface roughness analysis of TiB2 using copper electrodes, *J. Alloys Compd.* 690 (2017) 337–347.
- [119] H. S. Tak, C. S. HA, H. J. Lee, H. W. Lee, M. C. Kang, Characteristic evaluation of Al2O3/CNTs hybrid materials for micro-electrical discharge machining, *Trans. Nonferrous Met. Soc. China* 21 (1) (2011) 28–32.
- [120] M. A. Singh, D. K. Sarma, O. Hanzel, Surface characteristics enhancement of MWCNT alumina composites using multi-pass WEDM process, *J. Eur. Ceram. Soc.* 38 (11) (2018) 4035–4042.
- [121] M. A. Singh, S. K. Rajbongshi, D. Sarma, Surface and porous recast layer analysis in μ -EDM of MWCNT-Al2O3 composites, *Mater. Manuf. Processes* 34 (5) (2019) 567–579.
- [122] J. X. Deng, T. C. Lee, Techniques for improved surface integrity of electro discharge machined ceramic composites, *Surf. Eng.* 16 (5) (2000) 411–414.
- [123] Z. Zhu, V. G. Dhokia, A. Nassehi, A review of hybrid manufacturing processes-state of the art and future perspectives, *Int. J. Comput. Integ. M.* 26 (7) (2013) 596–615.
- [124] S. K. Chak, P. Rao, Trepanning of Al2O3 by electro-chemical discharge machining (ECDM) process using abrasive electrode with pulsed dc supply, *Int. J. Mach. Tool. Manu.* 47 (14) (2007) 2061–2070.
- [125] M. Goud, A. K. Sharma, C. Jawalkar, A review on material removal mechanism in electrochemical discharge machining (ECDM) and possibilities to enhance the material removal rate, *Precis. Eng.* 45 (2016) 1–17.
- [126] B. Bhattacharyya, B. Doloi, S. K. Sorkhel, Experimental investigations into electrochemical discharge machining (ECDM) of non-conductive ceramic materials, *J. Mater. Process. Technol* 95 (1-3) (1999) 145–154.
- [127] R. Ji, Y. Liu, Y. and Zhang, Compound machining of silicon carbide ceramics by high speed end electrical discharge milling and mechanical grinding, *Chinese Sci. Bull.* 57 (4) (2012) 421–434.
- [128] R. Ji, Y. Liu, Y. Zhang, Effect of machining parameters on surface integrity of silicon carbide ceramic using end electric discharge milling and mechanical grinding hybrid machining, *J. Mech. Sci. Technol* 27 (1) (2013) 177–183.
- [129] R. Baghel, H. S. Mali, S. K. Biswas, Parametric optimization and surface analysis of diamond grinding-assisted EDM of TiN-Al2O3 ceramic composite, *Int. J. Adv. Manuf. Tech.* 100 (2019) 1183–1192.
- [130] K. B. C., P. Rathod, J. B. Valaki, Ultrasonic vibrationassisted electric discharge machining: A research review, *Proc. Inst. Mech. Eng., Part B* 230 (2) (2016) 319–330.
- [131] Z. Zhang, H. Huang, W. Y. Ming, Study on machining characteristics of WEDM with ultrasonic vibration and magnetic field assisted techniques, *J. Mater. Process Technol* 234 (2016) 342–352.
- [132] T. B. Thoe, D. K. Aspinwall, N. Killey, Combined ultrasonic and electrical discharge machining of ceramic coated nickel alloy, *J. Mater. Process Technol* 92 (323–328).
- [133] C. Praneetpongprung, Y. Fukuzawa, S. Nagasawa, Effects of the edm combined ultrasonic vibration on the machining properties of Si3N4, *Mater. Trans.* 51 (11) (2010) 2113–2110.
- [134] A. Schubert, H. Zeidler, M. Hackert-Oschatzchen, J. Schneider, Enhancing micro-EDM using ultrasonic vibration and approaches for machining of nonconducting ceramics, *Stroj Veston-J Mech E* 59 (3) (2013) 156–164.
- [135] P. J. Liew, J. Yan, T. Kuriyagawa, Fabrication of deep micro-holes in reaction-bonded SiC by ultrasonic cavitation assisted micro-EDM, *Int. J. Mach. Tool. Manu.* 76 (2014) 13–20.
- [136] W. Y. Ming, Z. Zhang, S. Y. Wang, Comparative study of energy efficiency and environmental impact in magnetic field assisted and conventional electrical discharge machining, *J. Cleaner Prod.* 214 (2019) 12–28.
- [137] N. Rattan, R. S. Mulik, Experimental set up to improve machining performance of silicon dioxide (quartz) in magnetic field assisted TW-ECSM process, *Silicon* 10 (6) (2018) 2783–2791.
- [138] H. Gotoh, T. Tani, N. Mohri, Edm of insulating ceramics by electrical conductive surface layer control, *Procedia CIRP* 42 (2016) 201–205.
- [139] Z. Zhang, W. Y. Ming, H. Huang, Z. Chen, Z. Xu, Y. Huang, G. J. Zhang, Optimization of process parameters on surface integrity in wire electrical discharge machining of tungsten tool YG15, *Int. J. Adv. Manuf. Technol* 81 (5-8) (2015) 1303–1317.
- [140] B. Ekmekci, Residual stresses and white layer in electric discharge machining (EDM), *Appl. Surf. Sci.* 253 (23) (2007) 9234–9240.
- [141] A. Kumar, S. Maheshwari, C. Sharma, N. Beri, Analysis of machining characteristics in additive mixed electric discharge machining of nickel-based super alloy inconel 718, *Mater. Manuf. Processes* 26 (8) (2011) 1011–1018.
- [142] L. Li, R. X. Wang, M. Shen, Phase/domain structure and enhanced thermal stable ferro-/pyroelectric properties of (1-x) 0.94 Na0.48 Bi0.44 TiO3-0.06 BaTiO3: xZnO ceramics, *J. Eur. Ceram. Soc.* 40 (3) (2020) 699–705.
- [143] W. Ma, P. Fan, D. Salamon, Fine-grained BNT-based lead-free composite ceramics with high energy-storage density, *Ceram. Int.* 45 (16) (2019) 19895–19901.
- [144] W. Ma, P. Fan, D. Salamon, High discharged energy density of nanocomposites filled with double-layered core-shell nanoparticles by reducing space charge polarization, *Ceram. Int.* 44 (16) (2019) 19330–19337.
- [145] W. Y. Ming, J. Ma, Z. Zhang, H. Huang, D. L. Shen, G. J. Zhang, Y. Huang, **Soft computing models and intelligent optimization system in electro-discharge machining of SiC/Al composites**, *Int. J. Adv. Manuf. Tech.* 87 (1-4) (2016) 201–217.
- [146] Z. Zhang, H. S. Yu, Y. M. Zhang, K. Yang, W. Y. Li, Z. Chen, G. J. Zhang, **Analysis and optimization of process energy consumption and environmental impact in electrical discharge machining of titanium superalloys**, *J. Cleaner Prod.* 198 (PT.1-1652) (2018) 833–846.